

Locally Valid and Discriminative Prediction Intervals for Deep Learning Models

Zhen Lin

University of Illinois at Urbana-Champaign
Urbana, IL 61801
zhenlin4@illinois.edu

Shubhendu Trivedi

MIT
Cambridge, MA 02139
shubhendu@csail.mit.edu

Jimeng Sun

University of Illinois at Urbana-Champaign
Urbana, IL 61801
jimeng@illinois.edu

Abstract

Crucial for building trust in deep learning models for critical real-world applications is efficient and theoretically sound uncertainty quantification, a task that continues to be challenging. Useful uncertainty information is expected to have two key properties: It should be *valid* (guaranteeing coverage) and *discriminative* (more uncertain when the expected risk is high). Moreover, when combined with deep learning (DL) methods, it should be *scalable* and *affect the DL model performance minimally*. Most existing Bayesian methods lack frequentist coverage guarantees and usually affect model performance. The few available frequentist methods are rarely discriminative and/or violate coverage guarantees due to unrealistic assumptions. Moreover, many methods are expensive or require substantial modifications to the base neural network. Building upon recent advances in conformal prediction [13, 33] and leveraging the classical idea of kernel regression, we propose Locally Valid and Discriminative prediction intervals (LVD), a simple, efficient and lightweight method to construct discriminative prediction intervals (PIs) for almost *any* DL model. With no assumptions on the data distribution, such PIs also offer finite-sample local coverage guarantees (contrasted to the simpler marginal coverage). We empirically verify, using diverse datasets, that besides being the only locally valid method for DL, LVD also exceeds or matches the performance (including coverage rate and prediction accuracy) of existing uncertainty quantification methods, while offering additional benefits in scalability and flexibility.

1 Introduction

Consider a training set $\mathcal{S}_{\text{train}} = \{(X_i, Y_i)\}_{i=1}^N$ and a test example (X_{N+1}, Y_{N+1}) , all drawn i.i.d from an arbitrary joint distribution \mathcal{P} , with $(X_i, Y_i) \in \mathcal{X} \times \mathcal{Y}$ for some $\mathcal{X} \subseteq \mathbb{R}^d$ and $\mathcal{Y} \subseteq \mathbb{R}$. We are interested in the problem of predictive inference: On observing $\mathcal{S}_{\text{train}}$ and X_{N+1} , our task is to construct a prediction interval (PI) ¹ estimate $\hat{C}(X_{N+1})$ that contains the true value of Y_{N+1} with a (pre-specified) high probability.

¹Several recent deep learning papers use “Confidence Interval” and “Prediction Interval” interchangeably. We stick to the conventional statistical usage.

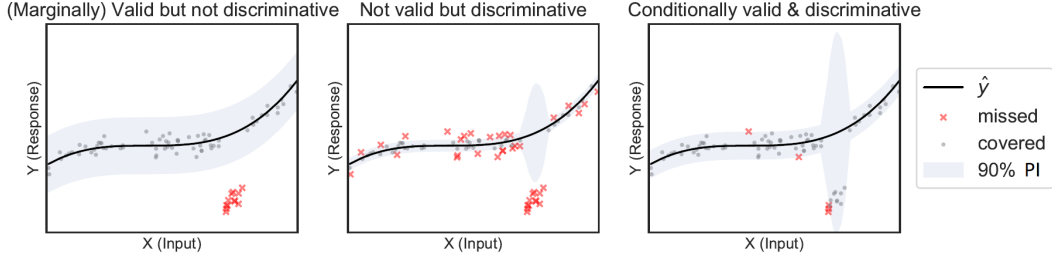


Figure 1: Illustration of possible (good and bad) PIs. The PI on the left is valid, as it covers 90% of the data. It is however only marginally valid, not reflecting the poor model prediction near the red cluster. The middle PI is discriminative, and reflects the high error near the red cluster, but its coverage rate is much lower than the target (thus not valid). The PI on the right addresses both challenges by stretching “just enough” near the cluster, making it not only discriminative, but also *conditionally* valid. We seek to construct PIs of the last type, but constructing exact conditionally valid PIs in a distribution-free setting is theoretically impossible. We thus relax this goal by instead aiming for local validity (more details in Section 2).

The construction of actionable PIs involves two *general challenges*: First, \hat{C} should be **valid**, meaning that if the specified probability is $1 - \alpha$, we expect $\hat{C}(X_{N+1})$ to cover Y_{N+1} at least $1 - \alpha$ of the time. Moreover, \hat{C} should be **discriminative** i.e., we expect $\hat{C}(X_{N+1})$ to be narrower for confident cases and vice-versa. The width of the PI $\hat{C}(X_{N+1})$ is thus quantification of the uncertainty. Figure 1 illustrates these notions, with more details in Section 2.2 and 2.3.

While deep learning (DL) models have demonstrated impressive performance over a range of complicated tasks and data modalities, it has remained difficult to quantify the uncertainty for their predictions. For DL predictions to be actionable, uncertainty information is however indispensable, especially in domains like medicine and finance [2]. Apart from requiring validity and discrimination as discussed earlier, two additional challenges exist *specifically* for DL models. Obviously, any uncertainty estimation method needs to finish reasonably fast to be useful, so the third challenge is *scalability*. The fourth challenge is *accuracy*: The uncertainty estimation should not decrease the prediction accuracy of the DL model. *Post-hoc* methods are ideal because they usually do not interfere with the base NN prediction at all. These four requirements together constitute a set of essential desiderata for uncertainty quantification in DL.

Existing uncertainty estimation methods for DL rarely address more than one or two of the above requirements. Credible intervals given by posteriors of approximate Bayesian methods such as [43, 15], deep ensemble [20, 44] and Monte-Carlo dropout [12] are not valid in the frequentist sense [7]. Most existing methods also interfere with the original model design, loss function and/or training, which could be expensive and decrease the model performance (as verified in our experiments) [12, 1, 7, 20].

To address these requirements, we leverage recent advances in conformal prediction and the classical idea of kernel regression. Conformal prediction, pioneered by Vovk [40], is a powerful approach for constructing valid PIs. The most popular split conformal methods usually leverage prediction errors from a hold-out set to construct $\hat{C}(X_{N+1})$, which would be valid if a future data point (X_{N+1}, Y_{N+1}) follows the same distribution as data in the hold-out set. This framework is particularly suitable for deep learning due to its distribution-free nature, and has motivated many recent uncertainty quantification efforts in deep learning for both classification and regression tasks [1, 23, 3, 11]. However, most conformal methods are only marginally valid [25, 40, 21, 4]. Moreover, less-than-meticulous applications to DL can break distributional assumptions and theoretical validity, as in the case of [1] (see discussion in Appendix). We however seek to construct a PI conditioning on the input (similar to the third PI in Fig. 1). Some recent advances ([13, 33]) examine the possibility of “approximately” conditionally valid PIs. While these methods cannot be directly applied to DL due to efficiency and performance considerations, their methodological and theoretical contributions serve as major inspirations for us to develop a highly flexible and practical method.

Summary of Contributions: We propose Locally Valid Discriminative Prediction Intervals (LVD), a simple uncertainty estimation method for deep learning which combines recent advances in conformal prediction and the classical idea of kernel regression. LVD applies to almost all DL models, and is the first method that satisfies all four aforementioned requirements:

- **Validity:** LVD has frequentist coverage guarantee (not just marginal, but approximately conditional).

- **Discrimination:** The width of the PIs given by LVD adapts to the risk/uncertainty level of X_{N+1} .
- **Scalability:** LVD is lightweight, adding limited overhead to the base DL model.
- **Accuracy:** LVD is post-hoc without requiring model retraining, and does not affect the base performance of the DL model.

We must note that while the theoretical foundation for guaranteeing "validity" is mostly based on [13], LVD addresses several challenges to satisfy the other three requirements. The code to replicate all our results can be found at <https://github.com/zlin7/LVD>.

2 Preliminaries

2.1 Learning Setup and Assumptions

We assume data and response pairs $(X, Y) \in \mathcal{X} \times \mathcal{Y}$ have a joint distribution denoted \mathcal{P} , with the marginal distributions of Y and X and the conditional distribution $Y|X$ denoted as \mathcal{P}_Y , \mathcal{P}_X , and $\mathcal{P}_{Y|X}$, respectively. Further, we will define $Z_i := (X_i, Y_i)$ for concision.

Assuming that we already have an algorithm (with all the training protocols folded in), such as a Deep Neural Network (DNN), that provides a mean estimator $\hat{\mu}^{NN}(x) : \mathcal{X} \mapsto \mathcal{Y}$. Given a target coverage level $1 - \alpha \in (0, 1)$, our task is to also construct a prediction interval estimator function $\hat{C}_\alpha(x) : \mathcal{X} \mapsto \{\text{subset of } \mathcal{Y}\}$ that has the **validity** and **discrimination** properties as defined below.

2.2 Validity (Frequentist Coverage)

There are several (related) notions for a PI to be valid – marginal, conditional, and local. Given target level $1 - \alpha$, we say \hat{C}_α has the **marginal coverage** guarantee (or, equivalently, is marginally valid) if

$$\mathbb{P}\{Y_{N+1} \in \hat{C}_\alpha(X_{N+1})\} \geq 1 - \alpha \quad (1)$$

where the probability is taken over the training data and (the unseen) (X_{N+1}, Y_{N+1}) .

A limitation of marginal coverage is that it is not conditioned on X_{N+1} . A more desirable, albeit stronger, property would be **conditional coverage** at $1 - \alpha$:

$$\mathbb{P}\{Y_{N+1} \in \hat{C}_\alpha(X_{N+1}) | X_{N+1} = x\} \geq 1 - \alpha \text{ for almost all } x \in \mathcal{X}. \quad (2)$$

Here the probability is taken over the training data and Y_{N+1} (with X_{N+1} fixed). It is thus clear that conditional coverage implies marginal coverage but not the other way around. Indeed, a \hat{C}_α with marginal coverage property only implies a $1 - \alpha$ chance of being accurate *on average* across all data points (marginalizing over X_{N+1}) i.e. there might be a sub-population in the data for which the coverage is completely missed. Unfortunately, it is *impossible* to achieve distribution-free finite-sample conditional coverage (Eq. 2) in a non-trivial way. Indeed, it is known that a finite-sample estimated $\hat{C}_\alpha(x)$ cannot achieve conditional coverage, unless it produces infinitely wide prediction intervals in expectation under any non-discrete distribution \mathcal{P} [39, 22, 5].

It is thus reasonable to instead seek **approximate** conditional coverage. As might be apparent, there is considerable freedom in defining an appropriate notion of "approximate", depending on specific tasks and domains. However, a sufficiently general-purpose and natural notion involves using a kernel function $K : \mathcal{X} \times \mathcal{X} \mapsto \mathbb{R}$ and a center $x' \in \mathcal{X}$, like the relaxation given in [33]:

$$\frac{\int \mathbb{P}\{Y_{N+1} \in \hat{C}_\alpha(x') | X_{N+1} = x\} K(x, x') d\mathcal{P}_X(x)}{\int K(x, x') d\mathcal{P}_X(x)} \geq 1 - \alpha \quad (3)$$

with the probability (\mathbb{P} in the integral) taken over all training samples and Y_{N+1} , with $(X_{N+1}, Y_{N+1}) \sim \tilde{\mathcal{P}} = \tilde{\mathcal{P}}_X \times \mathcal{P}_{Y|X}$. Here $\tilde{\mathcal{P}}_X$ is just the distribution re-weighted by the kernel with a center x' , defined by $\frac{d\tilde{\mathcal{P}}_X(x)}{dx} \propto \frac{d\mathcal{P}_X(x)}{dx} K(x', x)$. Instead of choosing x' beforehand, if we let the center be X_{N+1} and fold the integral into \mathbb{P} like in [13], we arrive at the definition of **local coverage**:

$$\mathbb{P}\{\tilde{Y}_{N+1} \in \hat{C}_\alpha(X_{N+1}) | X_{N+1} = x'\} \geq 1 - \alpha. \quad (4)$$

Here the probability integrates over all training data and an additional $(\tilde{X}_{N+1}, \tilde{Y}_{N+1}) \sim \tilde{\mathcal{P}}$ defined above. Intuitively, this definition means $\hat{C}_\alpha(X_{N+1})$ is valid "on average" within a small neighborhood

of X_{N+1} . Note that Eqs. 1 and 2 reduce to Eq. 4 with K being constant and delta functions, respectively. In the rest of the paper, we will call \hat{C}_α marginally/conditionally/locally valid if it satisfies Eq. 1/2/4 respectively, and we will pursue finite-sample **local validity**.

2.3 Discrimination

The idea of discrimination is simple: If the error of our prediction $\hat{\mu}(x)$ is high for an input x , the PI should be wide, and vice versa. Formally, following [1], we require

$$\mathbb{E}[W(\hat{C}(x))] \geq \mathbb{E}[W(\hat{C}(x'))] \Leftrightarrow \mathbb{E}[\ell(y, \hat{\mu}(x))] \geq \mathbb{E}[\ell(y', \hat{\mu}(x'))]. \quad (5)$$

Here the expectation is taken over the training data, W is a measure of the width of the PI, and ℓ is a loss function such as MSE. This property can be verified (as shown in Section 4) by checking how well $W(\hat{C}(x))$ could predict the magnitude of the error. Discrimination could be considered a measure of efficiency, as a good \hat{C} could “save” some width when the expected risk is low. However, it only makes sense to compare efficiency if all else is equal (i.e. two marginally valid PIs estimators with the same error). Note that although discrimination could be related to conditional/local validity, they are not the same - e.g., a PI that is always infinitely wide is conditionally valid, but not discriminative.

Our goal is to achieve both local validity and discrimination without making any assumptions about the underlying distribution \mathcal{P} (i.e., in a distribution-free setting). As noted in Section 1, our method should also run fast and not affect the performance of underlying neural network model $\hat{\mu}^{NN}$.

3 Method: Locally Valid Discriminative Prediction Intervals (LVD)

Overview: We first train a deep neural network (DNN) $\hat{\mu}^{NN}$ (if not already given), followed by a post-hoc training of an appropriately chosen kernel function K . Specifically, we learn K in a non-parametric kernel regression setting using embeddings from the deep learning model while optimizing for the underlying distance metric that the kernel function leverages. Both of these steps are explicated in more detail in Section 3.1. Armed with $\hat{\mu}^{NN}$, we proceed to utilize a hold-out set to collect prediction residuals, which are used with the learned K (along with its distance metric) to build the final PI for any datum at inference time (Section 3.2). We then show the finite-sample local validity and asymptotic conditional validity in Section 3.4.

3.1 Training

At the onset, we partition $\mathcal{S}_{\text{train}}$ of N data points into two sets - $\mathcal{S}_{\text{embed}}$ and $\mathcal{S}_{\text{conformal}}$. We will denote $\mathcal{S}_{\text{embed}}$ as $\{Z_i\}_{i=1}^n$ and $\mathcal{S}_{\text{conformal}}$ as $\{Z_{n+i}\}_{i=1}^m$, where $m = N - n$. $\mathcal{S}_{\text{embed}}$ is used to learn an embedding function \mathbf{f} and a kernel K , and $\mathcal{S}_{\text{conformal}}$ is used for conformal prediction.

[Optional] Training an Embedding Function: Instead of training a deep kernel in a kernel regression directly, which can be prohibitively expensive, we split the training task into two steps: training the (expensive) DNN, and training the kernel K . Specifically, we first train a DNN mean estimator $\hat{\mu}^{NN} : \mathcal{X} \mapsto \mathcal{Y}$ to solve the supervised regression task with the mean squared error (MSE) loss. Note that $\hat{\mu}^{NN}$ can be based on any existing model. Moreover, this step could be skipped if we are already provided with a pre-trained $\hat{\mu}^{NN}$. Then, we remove the last layer of $\hat{\mu}^{NN}$ and produce an embedding function $\mathbf{f} : \mathcal{X} \mapsto \mathbb{R}^h$ for some positive integer h . If the original model $\hat{\mu}^{NN}$ is good, usually such an embedding provides a rich and discriminative representation of the input (as will be verified empirically in Section 4).

Training the Kernel: Fixing the embedding function \mathbf{f} , we perform leave-one-out Nadaraya-Watson [24][14][41] kernel regression with a learnable Gaussian kernel on $\mathcal{S}_{\text{embed}}$:

$$\hat{g}_i^{KR} = \frac{\sum_{j \neq i, j \in [n]} y_j K_{\mathbf{f}}(x_i, x_j)}{\sum_{j \neq i, j \in [n]} K_{\mathbf{f}}(x_i, x_j)} \quad (6)$$

$$\text{where } K_{\mathbf{f}}(x_i, x_j) = K(\mathbf{f}(x_i), \mathbf{f}(x_j)) = \frac{1}{\sigma \sqrt{2\pi}} e^{-\frac{d(\mathbf{f}(x_i), \mathbf{f}(x_j))}{\sigma^2}} \text{ and } [n] := \{1, \dots, n\}. \quad (7)$$

Here $d(\cdot, \cdot)$ is a Mahalanobis distance parameterized by a positive-semidefinite matrix $\mathbf{W} \succeq 0$, which is learned. To avoid solving an expensive semi-definite program, instead of working with \mathbf{W} directly,

we work with a low-rank matrix $\mathbf{A} \in \mathbb{R}^{h \times k}$ such that $\mathbf{W} = \mathbf{A}^T \mathbf{A}$, yielding the following equivalent distance formulation:

$$d(\mathbf{f}(x_i), \mathbf{f}(x_j)) = \|\mathbf{A}(\mathbf{f}(x_i) - \mathbf{f}(x_j))\|^2. \quad (8)$$

This parameterization of K is similar to that in [42]. Finally, to train K , we minimize the MSE loss.

Residual Collection: In this step, we take the trained embedding function and kernel, denoted as $K_{\mathbf{f}}$ for simplicity, and apply it on $\mathcal{S}_{\text{conformal}}$. $\forall i \in [m]$, we compute and collect the absolute residual,

$$R_i = |y_{n+i} - \hat{y}_{n+i}|, \quad (9)$$

the distribution of which is used for PI construction. It is important to remark that \hat{y} does not have to be \hat{y}^{KR} . The main purpose of the previous step is to train the K , and \hat{y} could still be obtained through the original DNN $\hat{y} = \hat{\mu}^{NN}(x)$, or *any* estimator not trained on $\mathcal{S}_{\text{conformal}}$. As a result, the accuracy can only improve (if \hat{y}^{KR} turns out to be a better mean estimator)².

3.2 Inference

Before proceeding further, we recall a useful definition and fix some necessary notation. For a distribution with cumulative density function (cdf) F defined on the augmented real line $\mathbb{R} \cup \{-\infty, \infty\}$, the quantile function is defined as $Q(\alpha, F) = F^{-1}(\alpha)$. This definition is the same for a finite distribution like the empirical distribution. Suppose the empirical distribution consists of R_1, \dots, R_m , then we denote the empirical distribution \hat{F} and the empirical quantile $Q(\alpha, \hat{F})$ as:

$$\hat{F} = \frac{1}{m} \sum_{i=1}^m \delta_{R_i} \quad \text{and} \quad Q(\alpha, \hat{F}) = \inf_r \hat{F}(r) \geq \alpha \quad (10)$$

where $\delta_R(r) = \mathbb{1}\{r \geq R\}$. Note that we treat $\{R_i\}_{i=1}^m$ as an unordered list. Besides, R_i can be $\pm\infty$, and can repeat. Finally, we can assign weights to R_i , and define the quantiles for a weighted distribution:

$$\tilde{F} = \sum_{i=1}^m w_i \delta_{R_i} \quad \text{where} \quad \sum_{i=1}^m w_i = 1. \quad (11)$$

Split Conformal: Before presenting the detailed construction of the PI in LVD, it would be particularly instructive to first consider a special case. Specifically, when K returns a constant number for any (x_i, x_j) , we recover the well-known ‘‘split conformal’’ method [25, 40, 21], which uses the $1 - \alpha$ quantile of the residuals as the PI width. Following our setup, the split conformal PI is given by:

$$\hat{C}_{\alpha}^{\text{split}}(X_{N+1}) = \left\{ y \in \mathbb{R} : |y - \hat{y}_{N+1}| \leq Q \left(1 - \alpha, \frac{1}{m+1} \left(\delta_{\infty} + \sum_{i=1}^m \delta_{R_i} \right) \right) \right\}. \quad (12)$$

Because the residuals $\{R_i\}_{i \in [m]} \cup \{R_{N+1}\}$ are i.i.d., R_{N+1} ’s ranking among them is uniformly distributed. We cannot know R_{N+1} , so we use ∞ instead to be ‘‘safe’’ ($\forall r \in \mathbb{R}, \delta_{\infty}(r) = 0$). It follows that $\hat{C}_{\alpha}^{\text{split}}$ is $(1 - \alpha)$ marginally valid [25].

Local Conformal: In order to achieve the local coverage property, all we need to do is to re-weight the residuals. Following the approach in [13], we arrive at the following suitable notion of PI:

$$\hat{C}_{\alpha}^{LVD}(X_{N+1}) = \left\{ y \in \mathbb{R} : |y - \hat{y}_{N+1}| \leq Q \left(1 - \alpha, \left(w_{N+1} \delta_{\infty} + \sum_{i=1}^m w_{n+i} \delta_{R_i} \right) \right) \right\} \quad (13)$$

$$\text{where } w_j = \frac{K_{\mathbf{f}}(x_j, x_{N+1})}{K_{\mathbf{f}}(x_{N+1}, x_{N+1}) + \sum_{i=1}^m K_{\mathbf{f}}(x_{n+i}, x_{N+1})}. \quad (14)$$

In other words, we first assign weights to $\{R_i\}$ based on the similarity between $\{X_{n+i}\}$ and X_{N+1} using $K_{\mathbf{f}}$, and then set the width to be the weighted quantile. Note that with δ_{∞} , $\hat{C}_{\alpha}^{LVD}(X_{N+1})$ will be infinitely wide if data is scarce around X_{N+1} . However, as argued in [13], this is desired.

²As will be shown in the Appendix, \hat{y}^{KR} is often preferable because of the distance information it encodes.

3.3 Implementation Details

Parameterization and Training: Since \mathbf{A} is intricately linked to the computation of the weights assigned by the Gaussian kernel K (Eq. 8), it is implemented as $K(\mathbf{f}(x_i), \mathbf{f}(x_j)) = e^{-\|\mathbf{A}(\mathbf{f}(x_i) - \mathbf{f}(x_j))\|^2}$. In order to optimize for \mathbf{A} , we treat it as a usual linear layer in a neural network and perform gradient descent.

Smoothness Requirement: In the context of obtaining locally valid prediction intervals, a potential drawback of using the Nadaraya-Watson kernel regression framework is that the $K_{\mathbf{f}}$ will not meaningfully learn the similarity of any input with *itself*. For example, we can arbitrarily define $K_{\mathbf{f}}(x, x)$ to be *any* value, including ∞ . In the context of only regression, the fitted function’s performance will not change as long as there are no two identical x_i . With the Gaussian kernel, this issue is somewhat mitigated. However, during the training, the $K(x_i, x_i)$ can still be too high compared with $K(x_i, x_i + \epsilon)$, resulting in a less meaningful definition for local coverage. We could then enforce a regularization by replacing the \hat{y}_i in Eq. 6 with

$$\hat{y}_i^{KR} = \frac{\bar{y}_{-i} K_{\mathbf{f}}(x_i, x_i) + \sum_{j \neq i, j \in [n]} y_j K_{\mathbf{f}}(x_i, x_j)}{K_{\mathbf{f}}(x_i, x_i) + \sum_{j \neq i, j \in [n]} K_{\mathbf{f}}(x_i, x_j)} \quad \text{where } \bar{y}_{-i} = \frac{1}{n-1} \sum_{j \neq i, j \in [n]} y_j. \quad (15)$$

This can be considered an explicit bias term towards the (leave-one-out) sample mean. Empirically, we observe that enforcing this requirement is crucial to obtain meaningful and tight intervals. We direct the reader to the Appendix for a detailed ablation on its utility.

Complexity: To facilitate training, we use stochastic gradient descent instead of gradient descent with batch size denoted as B_1 . Furthermore, if the dataset size is prohibitively large, we can also randomly sample a subset of B_2 points $\{x_j\}_{j \neq i}$ to predict \hat{y}_i . The total complexity is $O(B_1 B_2 h k)$ where h and k , defined earlier, denote the dimensionality of the embedding before/after it is multiplied by \mathbf{A} . Note that $B_2 = O(1)$ or $o(N)$. The inference time for each data point can be improved from $O(B_2 h k)$ to $O(B_2 k + h k)$ by storing $\mathbf{A} x_j$ instead of \mathbf{A} and x_j separately.

Denoting the number of parameter of the base NN as P , since DL models are usually overparameterized, the additional training time for each descent could be comparable or shorter than training the base NN (depending on the relation between P and $B_2 h k$)³, and the additional inference time would be much shorter than that of the base NN model. In addition, most of these factors (especially B_2) can be easily parallelized. The full procedure is summarized below in Algorithm 1.

Algorithm 1 LVD

Input:

$\mathcal{S}_{\text{train}}$: A set of observations $\{Z_i = (X_i, Y_i)\}_{i=1}^N$

α : Parameter specifying (local) target coverage rate

X_{N+1} : Unseen data point

Output: A locally valid PI, $\hat{C}_\alpha(X_{N+1})$.

Training:

[Optional] Randomly split $\mathcal{S}_{\text{train}}$ into $\mathcal{S}_{\text{embed}}$ and $\mathcal{S}_{\text{conformal}}$. Denote $\mathcal{S}_{\text{conformal}}$ as $\{Z_{n+i}\}_{i=1}^m$

[Optional] Train a NN regression model $\hat{\mu}^{NN}$ on $\mathcal{S}_{\text{embed}}$.

Remove the last layer of $\hat{\mu}^{NN}$ to get an embedding function \mathbf{f}

Train \mathbf{A} on $\mathbf{f}(\mathcal{S}_{\text{embed}})$ in a Nadaraya-Watson kernel regression setting, with kernel $K_{\mathbf{f}}(x_1, x_2) = e^{-\|\mathbf{A}(\mathbf{f}(x_1) - \mathbf{f}(x_2))\|^2}$

Collect residuals $R_i = |y_{n+i} - \hat{y}_{n+i}|$ for $i \in [m]$

Inference:

Compute PI as $\hat{C}_\alpha(X_{N+1}) = \left\{ y \in \mathbb{R} : |y - \hat{y}_{N+1}| \leq Q \left(1 - \alpha, w_{N+1} \delta_\infty + \sum_{i=1}^m w_{n+i} \delta_{R_i} \right) \right\}$

where $w_j = \frac{K_{\mathbf{f}}(x_j, x_{N+1})}{K_{\mathbf{f}}(x_{N+1}, x_{N+1}) + \sum_{i=1}^m K_{\mathbf{f}}(x_{n+i}, x_{N+1})}$

³In practice, since \mathbf{f} is already well-trained, the training of $K_{\mathbf{f}}$ converges very fast.

3.4 Theoretical Guarantees

We conclude this section by showing that \hat{C}_α^{LVD} provides the local coverage property. We adapt Theorem 5.1 in [13] and results in [33] to our setting. The detailed proof is deferred to the Appendix:

Theorem 3.1. *Conditional on X_{N+1} , the PI obtained from Algorithm 1, $\hat{C}_\alpha^{LVD}(X_{N+1})$, satisfies*

$$\mathbb{P}\{\tilde{Y}_{N+1} \in \hat{C}_\alpha^{LVD}(X_{N+1}) | X_{N+1} = x'\} \geq 1 - \alpha \text{ for any } x' \quad (16)$$

where the probability is taken over all the training samples $\stackrel{i.i.d.}{\sim} \mathcal{P} = \mathcal{P}_{Y|X} \times \mathcal{P}_X$, and $(\tilde{X}_{N+1}, \tilde{Y}_{N+1})$ with distribution $\tilde{X}_{N+1} | X_{N+1} \sim \mathcal{P}_X^{X_{N+1}}$ and $\tilde{Y}_{N+1} | \tilde{X}_{N+1} \sim \mathcal{P}_{Y|X}$. Here $\mathcal{P}_X^{X_{N+1}}$ means the localized distribution with $\frac{d\mathcal{P}_X^{X_{N+1}}(x)}{dx} \propto \frac{d\mathcal{P}_X(x)}{dx} K_{\mathbf{f}}(X_{N+1}, x)$.

With some regularity assumptions like in [22], we can also obtain asymptotic conditional coverage:

Theorem 3.2. *With appropriate assumptions, \hat{C}^{LVD} is asymptotically conditional valid.*

The detailed assumptions, formal statement, and proof of Theorem 3.2 are deferred to the Appendix.

Remark: Roughly speaking, Theorem 3.1 tells us that the response Y of a new data point sampled “near” X_{N+1} will fall in our PI with high probability. Theorem 3.2 further states that, under suitable assumptions and enough data, \hat{C}^{LVD} also covers Y_{N+1} (i.e., no re-sampling) with high probability.

4 Experiments

Baselines: We compare LVD with the following baselines (with a qualitative comparison in Table 1):

1. *Discriminative Jackknife (DJ)* [1], which claims to be both discriminative and marginally valid but is neither (See Appendix C).
2. *Deep Ensemble (DE)* [20], which trains an ensemble of networks to estimate variance and mean.
3. *Monte-Carlo Dropout (MCDP)* [12], a popular bayesian method for NN that performs Dropout [31] at inference time for the predictive variance estimate.
4. *Probabilistic Backpropagation (PBP)* [15], a successful method to train Bayesian Neural Networks by computing a forward propagation of probabilities before a backward computation of gradients.
5. *Conformalized Quantile Regression (CQR)* [29], an efficient (narrow PI) marginally valid conformal method that takes *quantile* predictors instead of mean predictors. This comes with a huge cost: one needs to retrain the predictor for *each* α if more than one coverage level is desired.
6. *MAD-Normalized Split Conformal (MADSplit)* [21, 8], a variant of the well-known split-conformal method that requires an estimator for the mean absolute deviation (MAD), and performs conformal prediction on the MAD-normalized residuals.

In our experiments, PIs for non-valid methods are obtained from the quantile functions of the posterior for target coverage $1 - \alpha$ like in [1].

4.1 Synthetic Data

We will first examine the dynamics of different uncertainty methods with synthetic data. The formula we use is the same as in [15, 1]: $y = x^3 + \epsilon$. Here, $\epsilon \sim \mathcal{N}(0, 4^2)$, and x comes from $Unif[-1, 1]$ with probability 0.9, and half-normal distribution on $[1, \infty)$ with $\sigma = 1$ with probability 0.1. We used this \mathcal{P}_X to illustrate local validity. The results are shown in Figure 2. We observe that LVD, CQR, MADSplit, and DJ all achieve close to 90% coverage. However, LVD gives a more meaningful discriminative predictive band: Specifically, near the boundaries, it will give us wider intervals (sometimes ∞) because there is little similar data around, which is desirable for local validity. Although CQR and MADSplit can be discriminative, they are still only marginally valid, so we can see that despite the varying width, they actually get narrower when x is more eccentric, which is clearly an issue. DJ essentially gives PIs of constant width, as estimated from the quantile of the residuals. DE also does not give meaningful uncertainty estimates, giving almost constant PIs that

Table 1: Features of different methods. CQR and MADSplit achieve strict finite-sample *marginal* coverage. Unlike LVD, no baseline is locally valid. LVD, MADSplit and CQR are discriminative, DJ is not, and DE/CMDP/PBP are supposed to be but usually fail to in our experiment. Among the post-hoc methods, LVD and MADSplit have reasonable overhead, DJ’s overhead is usually $O(N)$ where N is the number of training data (and extremely large memory consumption). CQR is not post-hoc because its PI may not contain $\hat{\mu}^{NN}(X)$.

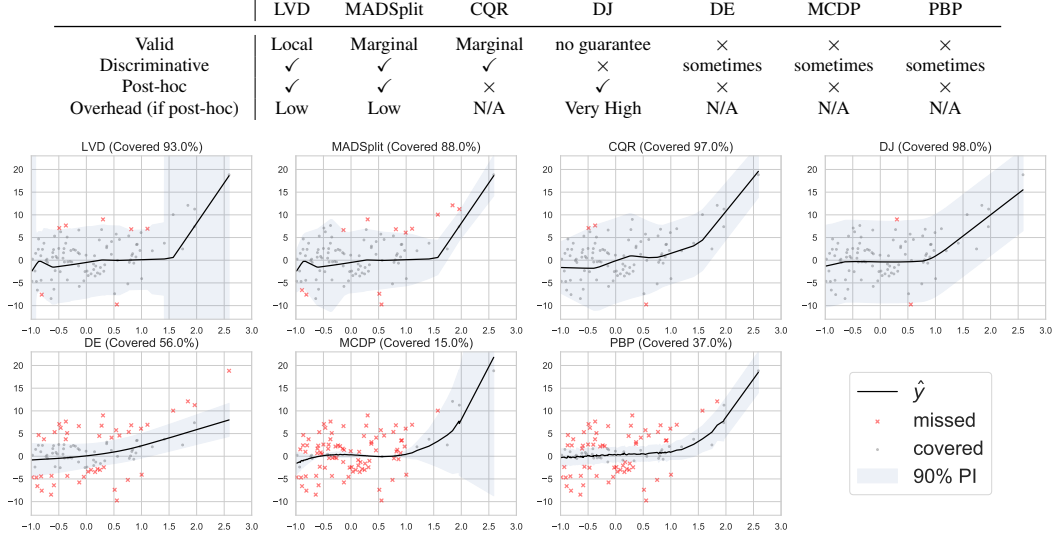


Figure 2: LVD, CQR and MADSplit achieve marginal coverage. Although without theoretical guarantee, DJ usually marginally covers in practice with near constant width (not discriminative). DE, MCDP and PBP do not show validity as expected. Among valid PIs, only LVD tries to capture the less representative points by wider PIs, arguably showing the most useful discriminative pattern.

cover well below 90%. For Bayesian methods, MCDP behaves much like a Gaussian Process (as claimed in [12]), with low coverage rate, whereas PBP is mildly discriminative and not valid⁴.

4.2 Real Datasets

Table 2: Size of each dataset. Size of the test set is in parenthesis.

Yacht	Housing	Energy	Bike	Kin8nm	Concrete	QM8	QM9
308 (62)	506 (101)	768 (154)	17379(3476)	8192 (1638)	1030 (206)	21786 (4357)	133719 (26744)

We will be using a series of standard benchmark datasets in the uncertainty literature [1, 29, 15], including: UCI Yacht Hydrodynamics (Yacht) [38], UCI Bikesharing (Bike) [35], UCI Energy Efficiency (Energy) [37], UCI Concrete Compressive Strength (Concrete) [36], Boston Housing (Housing) [9], Kin8nm [16]. We also use QM8 (16 sub-tasks) and QM9 (12 sub-tasks) [28, 30, 27] as examples of more complicated datasets. In each experiment, 20% of the data is used for testing. The sizes of datasets used are shown in Table 2. We use the same DNN model for all baselines, which has 2 layers, 100 hidden nodes each layer, and ReLU activation for the non-QM datasets. For QM8 and QM9, we use the molecule model implemented in [45] and apply applicable baselines. Missing baselines (“-” in the tables) are either too expensive (i.e. time and/or memory) or require a significant redesign of the training and NN, which is beyond the scope of this paper.

Evaluation Metrics: The evaluation is based on validity and discrimination. For validity, we check the marginal coverage rate (MCR) and the tail coverage rate (TCR), which is defined as the coverage rate for data whose Y falls in the top and bottom 10%. The motivation behind TCR is that if our local validity is very close to conditional validity, then LVD’s coverage rate would be above target in *any* pre-defined sub-samples, including those with extreme Y s. For discrimination, to verify Eq. 5, which

⁴Sometimes it may be possible to calibrate Bayesian methods [29]. However, one needs to calibrate the entire posterior for the Bayesian method to make sense. Moreover, from our experiments, it is impossible to do this in MCDP, when it behaves like a Gaussian process and predicts zero variance near known data.

is a prediction task, we compute the AUROC of using the PI width to predict whether the absolute residual is in the top half of all residuals. AUROC alone is misleading, however, as a bad predictor can easily be discriminative (e.g., by randomly adding to both its prediction and PI width a huge constant). Therefore, we also report the mean absolute deviation (MAD), defined as $\frac{\sum_{i=1}^M |\hat{y}_i - y_i|}{M}$.

Table 3: Marginal coverage rate (MCR) and tail coverage rate (TCR) (coverage rate for left and right 10% tail for test label) with target at 90%. “–” represents not-applicable models (see Section 4.2). Coverage rates not significantly lower than target at $p = 0.05$ are in bold (good). Note that the too high is not better. For example, MCDP either *greatly* over- or under-covers with MCR either 100% or well below 90%.

MCR	LVD	MADSplit	CQR	DJ	DE	MCDP	PBP
Yacht	96.8 ±2.2	82.4±7.1	91.5 ±4.7	95.0 ±2.1	22.7±6.0	87.4±4.2	80.2±10.8
Housing	96.8 ±2.9	90.6 ±3.5	91.7 ±3.3	97.6 ±1.4	96.0 ±1.9	100.0 ±0.0	8.1±4.3
Energy	94.0 ±1.6	90.3 ±2.5	90.3 ±2.2	96.2 ±1.8	98.0 ±2.7	100.0 ±0.0	7.2±5.9
Bike	90.4 ±0.8	89.9 ±0.6	89.8 ±0.7	95.2 ±0.6	100.0 ±0.0	71.9±0.7	0.6±0.2
Kin8nm	98.0 ±0.6	90.0 ±0.8	90.2 ±0.6	94.7 ±0.4	100.0 ±0.1	100.0 ±0.0	100.0 ±0.0
Concrete	97.4 ±1.3	88.8 ±2.8	88.5±2.3	98.0 ±1.6	97.8 ±1.0	100.0 ±0.0	3.3±0.8
QM8*	92.6 ±0.9	90.0 ±0.7	90.0 ±0.6	–	100.0 ±0.0	–	–
QM9*	90.3 ±0.6	90.0 ±0.2	90.0 ±0.3	–	60.7±46.8	–	–
TCR	LVD	MADSplit	CQR	DJ	DE	MCDP	PBP
Yacht	98.5 ±3.2	65.4±23.8	77.7±12.3	76.2±9.9	1.5±4.9	50.0±9.8	70.0±14.3
Housing	96.2 ±4.4	87.6 ±8.8	82.9±8.2	90.0 ±5.2	81.9±9.7	100.0 ±0.0	1.0±3.0
Energy	86.8 ±5.8	78.4±10.9	73.5±12.0	90.0 ±6.5	95.8 ±6.3	100.0 ±0.0	9.7±12.7
Bike	90.2 ±1.7	89.2 ±3.5	58.7±7.3	85.6±3.3	100.0 ±0.0	49.9±0.0	0.0±0.0
Kin8nm	97.2 ±1.6	86.4±2.6	85.2±2.2	88.1±1.8	99.9 ±0.3	100.0 ±0.0	100.0 ±0.0
Concrete	97.1 ±3.4	83.9±7.3	85.4±6.2	95.6 ±3.6	91.7 ±4.8	100.0 ±0.0	3.4±5.7
QM8*	90.8 ±1.9	86.3±2.4	80.0±5.9	–	100.0 ±0.0	–	–
QM9*	89.7 ±2.5	86.1±3.0	79.7±8.9	–	60.3±46.5	–	–

Table 4: At $p = 0.05$, AUROCs (in predicting error being greater than 50% percentile) that are significantly higher than 50%, and mean absolute deviations (MAD) significantly lower than the second-best, are in bold. LVD, MADSplit and CQR are consistently discriminative, but CQR sometimes incurs high MAD. DJ is not discriminative, whereas other methods occasionally demonstrate discrimination but usually have high MADs as well.

AUROC	LVD	MADSplit	CQR	DJ	DE	MCDP	PBP
Yacht	83.5 ±5.8	77.7 ±9.0	84.9 ±4.6	50.0±10.5	59.8 ±6.4	47.2±7.7	82.8 ±8.8
Housing	59.2 ±8.5	62.0 ±8.3	62.5 ±6.7	49.6±5.9	60.0 ±6.8	42.5±7.8	47.4±3.6
Energy	73.5 ±6.3	72.9 ±5.6	72.1 ±8.2	57.5 ±8.1	56.1±11.0	54.6 ±5.5	48.2±2.6
Bike	68.2 ±11.0	71.7 ±8.5	84.8 ±33.5	45.8±6.2	86.2 ±12.5	94.3 ±1.0	48.3±1.0
Kin8nm	60.3 ±1.1	60.4 ±1.9	60.0 ±2.1	49.3±2.2	50.5±2.6	54.1 ±2.5	53.6 ±4.8
Concrete	64.0 ±6.1	63.8 ±5.7	66.0 ±7.1	46.2±4.9	55.9 ±6.2	51.9±3.5	49.7±3.9
QM8*	71.3 ±9.4	73.5 ±6.8	65.5 ±10.3	–	91.7 ±16.9	–	–
QM9*	62.7 ±3.6	64.9 ±3.5	55.0 ±14.4	–	56.8 ±28.4	–	–
MAD	LVD	MADSplit	CQR	DJ	DE	MCDP	PBP
Yacht	1.90±0.48	1.90±0.48	3.55±0.85	10.15±0.84	11.25±0.81	10.92±0.73	1.80±0.30
Housing	3.31±0.53	3.31±0.53	3.44±0.33	3.69±0.33	4.42±0.39	6.04±0.54	7.94±1.97
Energy	2.99±0.75	2.99±0.75	3.44±1.04	3.19±0.51	3.79±0.31	8.12±0.59	11.66±2.24
Bike	0.04±0.03	0.04±0.03	7.34±3.51	0.05±0.03	3.37±2.90	124.57±2.68	162.21±2.58
Kin8nm	0.07 ±0.00	0.07 ±0.00	0.08±0.01	0.09±0.01	0.19±0.01	0.18±0.00	0.22±0.12
Concrete	5.44±0.53	5.44±0.53	6.21±1.05	5.58±0.58	7.22±0.76	13.75±0.69	20.59±3.57
QM8*	0.01 ±0.01	0.01 ±0.01	0.03±0.02	–	3.28±5.12	–	–
QM9*	3.69 ±9.09	3.69 ±9.09	32.11±50.42	–	268.32±357.01	–	–

We repeat all experiments 10 times and report mean and standard deviations. For QM8 and QM9, we report the average numbers across all sub-tasks, with a breakdown on each sub-task in the Appendix.

Results: For **validity**, as shown in Table 3, LVD achieves marginal coverage empirically, as well as MADSplit⁵, CQR, and DJ. However, for tail coverage rate, only LVD consistently covers at or above target coverage rates. For the larger datasets, both coverage rates tend to get close to 90% for LVD. DE, MCDP, and PBP do not achieve meaningful coverage (either too high or too low). [19] also report mixed results on marginal validity with existing uncertainty quantification methods for DL. To

⁵It is worth noting that MADSplit, despite the theoretical guarantee, misses on the Yacht dataset, because the MAD-predictor predicts a “negative” absolute residual for some subset of the data, thus creating extremely narrow PIs, even after requiring the prediction to be positive and the “practitioner’s trick” mentioned in [29].

further test for local validity, we also examine the average coverage rate conditioned on the presence of certain functional groups for the QM9 dataset (detailed results are relegated to the appendix). LVD achieves empirical validity for these groups as well, even though functional groups define a kind of similarity that is never used in the uncertainty quantification process.

For **discrimination** (Table 4), LVD is generally in the top two while maintaining the lowest MAD almost always. MADSplit has the same MAD as LVD (using the same $\hat{\mu}^{NN}$), and has a similar AUROC as LVD despite explicitly modeling MAD. Other baselines occasionally show a significant discriminative property, but usually have much higher MAD. Despite training an ensemble of models, DE incurs huge prediction errors in many datasets. As noted earlier, AUROC alone is misleading if the MAD is high: MCDP and CQR seem highly discriminative on the Bike dataset, mostly due to the high model error (epistemic uncertainty).

Scalability: For the largest dataset, QM9, the extra inference time of LVD vs. inference time of the original NN is 0.65 vs. 0.75 second per 1000 samples⁶ on an NVIDIA 2080Ti GPU. MADSplit on the other hand takes 0.93 second overhead in the most optimized case. That said, any method that finishes within $O(1)$ multiple of the original NN model is usable in practice. For LVD, extra vs. original training time is about 1.5 vs. 0.75 second per 1000 samples, but because the \mathbf{f} is already highly informative, the training of the kernel $K_{\mathbf{f}}$ finishes in very few iterations, resulting in $< 5\%$ overhead of the total training time. Note that MADSplit will take strictly $\geq 1\times$ time in total because it needs to train a second model to predict residuals. Like MADSplit, CQR needs to train at least one quantile predictor⁷, but it needs to train a new predictor for every α , which is a huge cost.

5 Conclusion

This paper introduces LVD, the first locally valid and discriminative PI estimator for DL, which is also scalable and post-hoc. Because LVD is both valid and discriminative, it can provide actionable uncertainty information for the real world application of DL regression models. Moreover, it is easy to apply LVD to almost any DL model without any negative impact on the accuracy due to its post-hoc nature. Our experiments confirm that LVD generates locally valid PIs that cover subgroups of data all other methods fail to. It also exceeds or matches the performance in discriminative power while offering additional benefits in scalability and flexibility. We foresee that LVD can enable more real-world applications of DL models by providing users actionable uncertainty information.

Acknowledgments

This work is in part supported by National Science Foundation award SCH-2014438, IIS-1418511, CCF-1533768, IIS-2034479, the National Institute of Health award NIH R01 1R01NS107291-01 and R56HL138415. The authors are also thankful to Andrew Gordon Wilson and three anonymous reviewers for their comments to help improve this work.

⁶We use the full $\mathcal{S}_{\text{conformal}}$ for PI construction, as the inference time is short enough without sampling.

⁷That is, if one is willing to have mean estimate outside the PI occasionally and consider CQR post-hoc.

References

- [1] Ahmed Alaa and Mihaela Van Der Schaar. Discriminative Jackknife: Quantifying Uncertainty in Deep Learning via Higher-Order Influence Functions. In Hal Daumé III and Aarti Singh, editors, *Proceedings of the 37th International Conference on Machine Learning*, volume 119 of *Proceedings of Machine Learning Research*, pages 165–174. PMLR, 2020.
- [2] Dario Amodei, Chris Olah, Jacob Steinhardt, Paul Christiano, John Schulman, and Dan Mané. Concrete problems in ai safety, 2016.
- [3] Anastasios Angelopoulos, Stephen Bates, Jitendra Malik, and Michael I. Jordan. Uncertainty sets for image classifiers using conformal prediction. *CoRR*, abs/2009.14193, 2020.
- [4] Rina Foygel Barber, Emmanuel J Candès, Aaditya Ramdas, and Ryan J Tibshirani. Predictive inference with the jackknife+. *The Annals of Statistics*, 49(1):486–507, 2021.
- [5] Rina Foygel Barber, Emmanuel J. Candès, Aaditya Ramdas, and Ryan J. Tibshirani. The limits of distribution-free conditional predictive inference. *arXiv*, abs/1903.04684, 2020.
- [6] Samyadeep Basu, Philip Pope, and Soheil Feizi. Influence Functions in Deep Learning Are Fragile, 2021.
- [7] M. J. Bayarri and J. O. Berger. The Interplay of Bayesian and Frequentist Analysis. *Statistical Science*, 19(1):58 – 80, 2004.
- [8] Anthony Bellotti. Constructing normalized nonconformity measures based on maximizing predictive efficiency. In Alexander Gammerman, Vladimir Vovk, Zhiyuan Luo, Evgeni Smirnov, and Giovanni Cherubin, editors, *Proceedings of the Ninth Symposium on Conformal and Probabilistic Prediction and Applications*, volume 128 of *Proceedings of Machine Learning Research*, pages 41–54. PMLR, 09–11 Sep 2020.
- [9] The boston housing dataset. <http://lib.stat.cmu.edu/datasets/boston>. Accessed: 2021-05-27.
- [10] Hadi Fanaee-T and Joao Gama. Event labeling combining ensemble detectors and background knowledge. *Progress in Artificial Intelligence*, pages 1–15, 2013.
- [11] Adam Fisch, Tal Schuster, Tommi S. Jaakkola, and Regina Barzilay. Efficient conformal prediction via cascaded inference with expanded admission. In *International Conference on Learning Representations*, 2021.
- [12] Yarin Gal and Zoubin Ghahramani. Dropout as a Bayesian approximation: Representing model uncertainty in deep learning. In *33rd International Conference on Machine Learning, ICML 2016*, 2016.
- [13] Leying Guan. Conformal prediction with localization. *arXiv*, abs/1908.08558, 2020.
- [14] László Györfi, Michael Kohler, Adam Krzyżak, and Harro Walk. *A Distribution-Free Theory of Nonparametric Regression*. Springer Science & Business Media, 2006.
- [15] José Miguel Hernández-Lobato and Ryan P. Adams. Probabilistic backpropagation for scalable learning of bayesian neural networks. In Francis R. Bach and David M. Blei, editors, *Proceedings of the 32nd International Conference on Machine Learning, ICML 2015, Lille, France, 6-11 July 2015*, volume 37 of *JMLR Workshop and Conference Proceedings*, pages 1861–1869. JMLR.org, 2015.
- [16] Kin family of datasets. <http://www.cs.toronto.edu/~delve/data/kin/desc.html>. Accessed: 2021-05-27.
- [17] Diederik P. Kingma and Jimmy Ba. Adam: A method for stochastic optimization. In Yoshua Bengio and Yann LeCun, editors, *3rd International Conference on Learning Representations, ICLR 2015, San Diego, CA, USA, May 7-9, 2015, Conference Track Proceedings*, 2015.
- [18] Pang Wei Koh and Percy Liang. Understanding black-box predictions via influence functions. In Doina Precup and Yee Whye Teh, editors, *Proceedings of the 34th International Conference on Machine Learning*, volume 70 of *Proceedings of Machine Learning Research*, pages 1885–1894. PMLR, 06–11 Aug 2017.
- [19] Benjamin Kompa, Jasper Snoek, and Andrew Beam. Empirical frequentist coverage of deep learning uncertainty quantification procedures. *CoRR*, abs/2010.03039, 2020.

- [20] Balaji Lakshminarayanan, Alexander Pritzel, and Charles Blundell. Simple and scalable predictive uncertainty estimation using deep ensembles. In *Advances in Neural Information Processing Systems*, 2017.
- [21] Jing Lei, Max G’Sell, Alessandro Rinaldo, Ryan J. Tibshirani, and Larry Wasserman. Distribution-Free Predictive Inference for Regression. *Journal of the American Statistical Association*, 2018.
- [22] Jing Lei and Larry Wasserman. Distribution-free prediction bands for non-parametric regression. *Journal of the Royal Statistical Society: Series B (Statistical Methodology)*, 76(1):71–96, 2014.
- [23] Zhen Lin, Cao Xiao, Lucas Glass, M. Brandon Westover, and Jimeng Sun. SCRIB: set-classifier with class-specific risk bounds for blackbox models. *CoRR*, abs/2103.03945, 2021.
- [24] Elizbar Nadaraya. *Nonparametric Estimation of Probability Densities and Regression Curves*. Kluwer Academic Publishers, 1989.
- [25] Harris Papadopoulos, Kostas Proedrou, Volodya Vovk, and Alex Gammerman. Inductive confidence machines for regression. In Tapio Elomaa, Heikki Mannila, and Hannu Toivonen, editors, *Machine Learning: ECML 2002*, pages 345–356, Berlin, Heidelberg, 2002. Springer Berlin Heidelberg.
- [26] Adam Paszke, Sam Gross, Francisco Massa, Adam Lerer, James Bradbury, Gregory Chanan, Trevor Killeen, Zeming Lin, Natalia Gimelshein, Luca Antiga, Alban Desmaison, Andreas Kopf, Edward Yang, Zachary DeVito, Martin Raison, Alykhan Tejani, Sasank Chilamkurthy, Benoit Steiner, Lu Fang, Junjie Bai, and Soumith Chintala. Pytorch: An imperative style, high-performance deep learning library. In H. Wallach, H. Larochelle, A. Beygelzimer, F. d’Alché-Buc, E. Fox, and R. Garnett, editors, *Advances in Neural Information Processing Systems 32*, pages 8024–8035. Curran Associates, Inc., 2019.
- [27] Raghunathan Ramakrishnan, Pavlo O Dral, Matthias Rupp, and O Anatole von Lilienfeld. Quantum chemistry structures and properties of 134 kilo molecules. *Scientific Data*, 1, 2014.
- [28] Raghunathan Ramakrishnan, Mia Hartmann, Enrico Tapavicza, and O. Anatole von Lilienfeld. Electronic spectra from tddft and machine learning in chemical space. *The Journal of Chemical Physics*, 143(8):084111, 2015.
- [29] Yaniv Romano, Evan Patterson, and Emmanuel Candes. Conformalized quantile regression. In H. Wallach, H. Larochelle, A. Beygelzimer, F. d’Alché-Buc, E. Fox, and R. Garnett, editors, *Advances in Neural Information Processing Systems*, volume 32. Curran Associates, Inc., 2019.
- [30] Lars Ruddigkeit, Ruud van Deursen, Lorenz C. Blum, and Jean-Louis Reymond. Enumeration of 166 billion organic small molecules in the chemical universe database gdb-17. *Journal of Chemical Information and Modeling*, 52(11):2864–2875, 2012. PMID: 23088335.
- [31] Nitish Srivastava, Geoffrey Hinton, Alex Krizhevsky, Ilya Sutskever, and Ruslan Salakhutdinov. Dropout: A simple way to prevent neural networks from overfitting. *Journal of Machine Learning Research*, 15(56):1929–1958, 2014.
- [32] Sul and Elena Chow. Globalchem: A content variable store for chemistry! <https://github.com/Sulstice/global-chem>, 2021.
- [33] Ryan J. Tibshirani, Rina Foygel Barber, Emmanuel J. Candes, and Aaditya Ramdas. Conformal prediction under covariate shift, 2020.
- [34] Athanasios Tsanas and Angeliki Xifara. Accurate quantitative estimation of energy performance of residential buildings using statistical machine learning tools. *Energy and Buildings*, 49:560–567, 2012.
- [35] Bike sharing data set. <https://archive.ics.uci.edu/ml/datasets/Bike+Sharing+Dataset>. Accessed: 2021-05-27.
- [36] Concrete compressive strength data set. <http://archive.ics.uci.edu/ml/datasets/concrete+compressive+strength>. Accessed: 2021-05-27.
- [37] Energy efficiency data set. <https://archive.ics.uci.edu/ml/datasets/energy+efficiency>. Accessed: 2021-05-27.
- [38] Yacht hydrodynamics data set. <http://archive.ics.uci.edu/ml/datasets/yacht+hydrodynamics>. Accessed: 2021-05-27.

- [39] Vladimir Vovk. Conditional validity of inductive conformal predictors. In Steven C. H. Hoi and Wray Buntine, editors, *Proceedings of the Asian Conference on Machine Learning*, volume 25 of *Proceedings of Machine Learning Research*, pages 475–490, Singapore Management University, Singapore, 04–06 Nov 2012. PMLR.
- [40] Vladimir Vovk, Alexander Gammernan, and Glenn Shafer. *Algorithmic learning in a random world*. Springer US, 2005.
- [41] Geoffrey S. Watson. Smooth regression analysis. *Sankhyā: The Indian Journal of Statistics, Series A (1961-2002)*, 26(4):359–372, 1964.
- [42] Kilian Q. Weinberger and Gerald Tesauero. Metric learning for kernel regression. In Marina Meila and Xiaotong Shen, editors, *Proceedings of the Eleventh International Conference on Artificial Intelligence and Statistics*, volume 2 of *Proceedings of Machine Learning Research*, pages 612–619, San Juan, Puerto Rico, 21–24 Mar 2007. PMLR.
- [43] Max Welling and Yee Whye Teh. Bayesian learning via stochastic gradient langevin dynamics. In *Proceedings of the 28th International Conference on Machine Learning, ICML 2011*, 2011.
- [44] Andrew Gordon Wilson and Pavel Izmailov. Bayesian deep learning and a probabilistic perspective of generalization. In Hugo Larochelle, Marc’Aurelio Ranzato, Raia Hadsell, Maria-Florina Balcan, and Hsuan-Tien Lin, editors, *Advances in Neural Information Processing Systems 33: Annual Conference on Neural Information Processing Systems 2020, NeurIPS 2020, December 6-12, 2020, virtual*, 2020.
- [45] Kevin Yang, Kyle Swanson, Wengong Jin, Connor Coley, Philipp Eiden, Hua Gao, Angel Guzman-Perez, Timothy Hopper, Brian Kelley, Miriam Mathea, Andrew Palmer, Volker Settels, Tommi Jaakkola, Klavs Jensen, and Regina Barzilay. Analyzing Learned Molecular Representations for Property Prediction. *Journal of Chemical Information and Modeling*, 59(8):3370–3388, 2019.
- [46] I.-C. Yeh. Modeling of strength of high-performance concrete using artificial neural networks. *Cement and Concrete Research*, 28(12):1797–1808, 1998.

A Proofs

A.1 Proof for Theorem 3.1

In this section, we will prove Theorem 3.1. The key idea behind the proof is that since $\hat{\mu}$ (let it be $\hat{\mu}^{NN}$ or $\hat{\mu}^{KR}$) and K_f are independent of $\mathcal{S}_{\text{conformal}}$, the residuals (R_i) collected on $\mathcal{S}_{\text{conformal}}$ follow the same distribution as a new test residual. Thus, re-weighting \mathcal{P}_X by K_f precisely fits into the covariate-shift setting studied by [33] (further studied in [13]), which in turn implies that under the new (localized) distribution for X , the coverage guarantee holds (Theorem 3.1).

We first introduce a few definitions following the same notation as in [13]. To begin, we define the score function as $V(x, y) := |y - \hat{\mu}(x)|$. Then, we write the localizer function as $H(x, x') := K_f(x, x')$. For convenience, we also will rewrite subscripts of the data, so we have $Z'_1 = (X'_1, Y'_1), \dots, Z'_{m+1} = (X'_{m+1}, Y'_{m+1})$, where Z'_i is just Z_{n+i} for $i \in [m]$ and Z'_{m+1} is Z_{N+1} . For $\{Z'_i\}_{i=1}^{m+1}$, both V and H would be considered *fixed* because the training did not use any information from $\mathcal{S}_{\text{conformal}}$. [13] allows for a more general form of H that can depend on $\mathcal{S}_{\text{conformal}}$, which is not needed in our setting.

We proceed to define the weighted residual distributions like in [13]:

$$\hat{\mathcal{F}}_i := \sum_{j=1}^{m+1} p_{i,j}^H \delta_{V(X'_j, Y'_j)} \quad (17)$$

$$\text{where } p_{i,j}^H := \frac{H(X'_i, X'_j)}{\sum_{k=1}^{m+1} H(X'_i, X'_k)} \quad (18)$$

Finally, $\hat{\mathcal{F}}$ is defined as $p_{m+1,m+1}^H \delta_\infty + \sum_{i=1}^m p_{m+1,i}^H \delta_{V(X'_i, Y'_i)}$. $V(X'_{m+1}, Y'_{m+1})$ can be considered set to ∞ , because we don't know the value of Y'_{m+1} and want to be conservative.

Now, our construction of the PI could be rewritten in the following form:

$$\hat{C}_\alpha^{LVD}(X'_{m+1}) := \{y : V(X'_{m+1}, y) \leq Q(1 - \alpha, \hat{\mathcal{F}})\} \quad (19)$$

This is precisely the setup of Theorem 5.1 in [13], and Theorem 3.1 follows from Theorem 5.1 in [13].

A.2 Asymptotic Conditional Validity (Theorem 3.2)

Before we discuss the asymptotic property of \hat{C}^{LVD} , we formally define asymptotic conditional validity (from [22]).

Definition 1. (*Asymptotic Conditional Validity*) Given training data $(X_1, Y_1), \dots, (X_m, Y_m)$, a PI estimator $\hat{C}_{m,\alpha}$ is asymptotically conditionally valid if

$$\sup_x \left[\mathbb{P}\{Y_{m+1} \notin C_{m,\alpha}(x) | X_{m+1} = x\} - \alpha \right]_+ \xrightarrow{\mathcal{P}} 0 \quad (20)$$

as $m \rightarrow \infty$, where the sup is taken over the support of \mathcal{P}_X .

Here, we add the subscript m to \hat{C}_α to emphasize the dependence on the sample size. If a PI estimator is asymptotically conditionally valid at level $1 - \alpha$, then given enough samples (as $m \rightarrow \infty$), the probability of $\hat{C}_{m,\alpha}$ missing the next response Y_{m+1} converges to α in probability. Note that LVD has an implicit assumption that the embedding function f (after some transformation) maps similar data close together. But with Theorem 3.2 such an assumption is not critical as the size of the dataset increases.

To facilitate the discussion, we add a subscript m and denote the PI given by LVD as $\hat{C}_{m,\alpha}^{LVD}$. With the setup mentioned in Section A.1, we obtain a result similar to Theorem 5.1 (b) in [13] to for $\hat{C}_{m,\alpha}^{LVD}$ as well.

Assumptions: We need to make the following assumptions:

- (1) Denote $W := \mathbf{f}(X)$ as a new random variable in \mathbb{R}^h . W is (assumed to be) on $[0, 1]^h$ with marginal density bounded from two sides by two constants $b_1 < b_2$. In other words, $0 < b_1 \leq p_W(w) \leq b_2 < \infty$.
- (2) The conditional density of R (the residual) given W is Lipschitz in W . In other words, $\forall w, w'$, $\|p_{R|W}(\cdot|w) - p_{R|W}(\cdot|w')\|_\infty \leq L\|w - w'\|$.

As might be clear, (1) and (2) are standard regularity assumptions (as in [13, 22]), but stated for our setting. For assumption (1), if W does not fall in $[0, 1]^h$, we can easily fix it by adding a normalization layer to \mathbf{f} . Compared with [13, 22], (2) is not any less likely to hold, as we usually only have one linear layer after \mathbf{f} in $\hat{\mu}^{NN}$.

Bandwidth (h): To clearly state the theorem, we also need to decompose/unfold our transform matrix \mathbf{A} into two steps - projection and rescaling: $\mathbf{A}(w - w') := \frac{1}{h} \mathbf{A}_1(w - w')$, where $\|\mathbf{A}_1\|_2 = 1$. Note that in our learning, we are mostly learning \mathbf{A}_1 , and h is in fact *chosen*. In our experiment, we implicitly folded h into \mathbf{A} , as changing h entails making an explicit decision on how “local” one wants the coverage to be when the data is limited, and we do not have a strong prior on this. However, for the sake of this discussion, as $N \rightarrow \infty$, if we keep the same ratio between $n = |\mathcal{S}_{\text{embed}}|$ and $m = |\mathcal{S}_{\text{conformal}}|$, then:

- \mathbf{A}_1 would converge to some fixed unit-norm matrix in $\mathbb{R}^{h \times k}$, and
- we could let $h \rightarrow 0$ like in [13] and [22], because if we have $m \rightarrow \infty$, then the number of validation residuals is large, so we could afford a much more “local” validity with few infinitely wide PIs.

With the assumptions stated above, we are in a position to state the following theorem regarding the asymptotic conditional validity of $\hat{C}_{m,\alpha}^{LVD}$:

Theorem A.1. (*Asymptotic Conditional Validity. Re-statement of Theorem 3.2*): *With assumptions (1) and (2), and $m \rightarrow \infty$, if we also let $h \rightarrow 0$, then*

$$\left[\alpha - \mathbb{P}\{Y'_{m+1} \in \hat{C}_{m,\alpha}^{LVD}(X'_{m+1})\} \right]_+ \xrightarrow{\mathcal{P}} 0. \quad (21)$$

The proof is essentially the same as that in [13], with the key difference that in [13], the Gaussian kernel only has one bandwidth h , which goes to 0 asymptotically. This has been discussed in the “Bandwidth (h)” section above. Note the key difference between Theorem A.1 and 3.1 is that the response Y'_{m+1} now belongs to X'_{m+1} , which is used to construct the PI.

B Additional Experimental Details

B.1 Training Details

As noted in the paper, the DNN used for most datasets (except QM8 and QM9) has 2 layers, 100 hidden nodes, and uses ReLU for the activation function. This is the same architecture as in [1], but with the difference that the activation is ReLU instead of tanh. We make this choice because the code accompanying [1] uses ReLU, and tanh does not train for most of the datasets in our experiments. Recall that the learnable matrix \mathbf{A} reduces dimension from h to k . For QM8 and QM9, please refer to [45] for a detailed description of the architecture and training protocols. We make the following modifications in order to run some baselines:

- MADSplit: We train a second model after the model in [45] that has the same architecture and training protocol, but tries to predict the absolute error of the first model.
- CQR: We replace the MSE loss with the “pinball” loss mentioned in [29] and simultaneously train two quantiles for the same α . For different α , we re-train a model.
- DE: We replace the loss with the negative log-likelihood (NLL) loss as suggested in [20], and train an ensemble of 5 models for each experiment.

For all experiments, h is given by the DNN, and we set $k = 10$. The training of the kernel follows the following protocol: we first take embedding from the training data, compute and fix the mean μ_i and standard deviation s_i for each dimension $i \in [h]$. Dimensions with standard deviation $< 1e-3$ are ignored as they are most likely dead nodes (due to ReLU). The embeddings are then always normalized using μ_i and s_i before passing through \mathbf{A} .

\mathbf{A} is implemented as a `torch.nn.Linear` layer using PyTorch[26] and follows the default initialization. We restrict the kernel regression to use the top 3000 (or all) similar data points so the computation can be fast (like in [42]). We use an Adam optimizer [17] implemented in PyTorch, with a learning rate set to $1e-2$, and batch size 100. We repeat the process for 1000 up to batches, and stop early if the loss does not improve for 50 consecutive batches.

For each setup, we repeat the experiment 10 times by randomly re-splitting training, validation, and test set with random seed from 0 to 9. For LVD, MADSplit, and CQR (which require a hold-out set for conformal prediction), we use 60% for training, 20% for validation/hold-out set, and 20% for test. For all other methods, we use 80% for training and 20% for testing.

B.2 Average PI Width

It is hard to compare efficiency because LVD achieves a much more demanding type of coverage, MADSplit and CQR achieve marginal coverage, and the rest of the methods are not valid (thus not comparable). We thus restrict the comparison to only valid methods (LVD, MADSplit, and CQR) and the subset of data for which all PIs are finite in Table 5. We can see that, as expected, LVD tends to give infinite PI for small datasets at 90% target level (“# finite” is low for a few datasets), because it requires some weighted observation in a local neighborhood. (Note that the # of finite PIs could be tuned by a bandwidth h as discussed in Section A.2.) However, despite providing a stronger coverage guarantee, LVD still managed to be the most efficient on Bike and QM9.

The most efficient method seems to be CQR, but the results are not very stable (very wide PIs for CQR in the Bike dataset, for example), and most of the time the difference in average width is not significant. However, as noted earlier in the main text, the potential efficiency of CQR comes with a huge cost: CQR requires re-training the model for each α . Moreover, there is no guarantee that the estimate of the lower bound of the PI is actually lower than the upper bound (“quantile crossing”, see [29]), nor that a mean estimate actually falls in the PI either. In our experiments, we had to take the mean of the lower and upper bound as the mean estimator to ensure the mean estimator is always within the PI.

We also include the average width of all baselines in Table 6 for reference, although it is not very meaningful to compare valid and non-valid methods.

Table 5: Average width of different conformal methods. Width significantly shorter than the second-best at $p = 0.05$ are in bold.

Data (Count)	# finite	50%-PI Width			# finite	90%-PI Width		
		LVD	MADSplit	CQR		LVD	MADSplit	CQR
Yacht(62)	61.90±0.32	3.99±0.79	3.17±0.84	2.82±0.74	40.90±2.85	3.47±1.36	3.29±1.04	4.52±2.08
Housing(101)	98.30±3.06	6.70±0.97	6.02±1.23	4.98 ±0.72	69.00±19.11	15.94±2.62	16.81±7.44	13.70 ±1.84
Energy(154)	154.00±0.00	6.06±1.41	5.77±1.37	5.18±1.47	145.10±11.05	12.89±2.02	12.19±2.71	13.76±2.80
Bike(3476)	3475.20±1.23	0.06±0.05	0.07±0.05	5.62±4.41	3467.50±4.40	0.15±0.13	0.19±0.11	33.65±21.52
Kin8nm(1638)	1610.10±10.18	0.14±0.01	0.12±0.01	0.12±0.01	938.00±123.72	0.34±0.02	0.28±0.02	0.28±0.02
Concrete(206)	200.10±4.01	10.92±1.85	9.77±1.66	9.35±2.84	133.80±20.13	27.93±3.59	21.79±2.93	22.87±3.48
QM8*(4357)	4317.33±22.90	0.02±0.01	0.02±0.01	0.04±0.01	4041.63±136.85	0.05±0.03	0.05±0.03	0.11±0.03
QM9*(26744)	26616.72±39.77	5.12±13.17	5.75±14.78	37.32±65.01	26146.95±151.58	15.06±38.94	14.77±37.04	129.63±207.46

Table 6: Average width of all baselines methods, without restriction to the subsample for which LVD gives finite PIs.

Width @ 50%	MADSplit	CQR	DJ	DE	MCDP	PBP
Yacht	3.18±0.82	2.83±0.72	19.10±1.26	5.26±0.78	14.34±0.71	2.16±0.31
Housing	6.06±1.22	5.00±0.71	11.50±1.41	10.23±1.50	30.58±0.33	0.74±0.08
Energy	5.77±1.37	5.18±1.47	9.83±1.39	10.52±1.59	30.14±0.24	0.78±0.04
Bike	0.07±0.05	5.62±4.41	0.14±0.07	13.62±6.61	115.47±0.84	0.84±0.27
Kin8nm	0.12±0.01	0.12±0.01	0.25±0.02	0.80±0.03	0.98±0.02	1.29±0.14
Concrete	9.84±1.70	9.39±2.82	47.98±84.01	18.33±2.96	47.82±0.30	0.78±0.06
QM8*	0.05±0.03	0.11±0.03	—	42.17±28.01	—	—
QM9*	14.77±37.04	129.63±207.46	—	465.17±919.56	—	—

Width @ 90%	MADSplit	CQR	DJ	DE	MCDP	PBP
Yacht	8.02±0.98	12.31±1.79	73.14±1.75	13.13±1.24	34.96±1.73	5.26±0.77
Housing	18.71±9.91	15.10±1.79	26.31±1.87	24.97±2.58	74.57±0.81	1.82±0.19
Energy	12.24±2.78	13.75±2.88	18.54±2.10	25.65±5.58	73.50±0.60	1.91±0.09
Bike	0.19±0.11	33.96±21.87	0.32±0.18	38.50±13.26	281.24±1.66	2.04±0.65
Kin8nm	0.31±0.02	0.32±0.01	0.48±0.03	1.89±0.15	2.39±0.06	3.15±0.35
Concrete	22.52±2.93	23.29±3.32	199.19±369.33	44.02±4.73	116.62±0.74	1.90±0.16
QM8*	0.05±0.03	0.11±0.03	—	42.17±28.01	—	—
QM9*	14.77±37.04	129.63±207.46	—	465.17±919.56	—	—

B.3 Additional Results of Different Variants of LVD

Although we consider MADSplit as a baseline, our method could be combined with it as well, by simply replacing R_i with a normalized $R'_i := \frac{y_{n+i} - \hat{y}_{n+i}}{\hat{\sigma}(x_{n+i})}$ like that in MADSplit. One key observation is that using embedding given by a pre-trained DL model can simultaneously keep most of the performance of the base model and combine it with many conformal methods with acceptable overhead.

In this section, we will change different settings of LVD and compare the effects. Specifically, there are 3 independent choices:

- Whether we use the kernel regression prediction \hat{y}^{KR} or the base DNN predictor $\hat{\mu}^{NN}$ (KR vs. NN)
- Whether we apply the smoothness requirement as mentioned in Section 3.3 (No-smooth vs. Smooth)
- Whether we normalize the residuals by an extra prediction of MAD or not. We will denote the version described in the main text as “base”. For the MAD-Normalized case (“MN”), similar to MADSplit [21, 8], the non-conformity score, and the final PI construction, are replaced by

$$R'_i := \frac{y_{n+i} - \hat{y}_{n+i}}{\hat{\sigma}(x_{n+i})} \quad (22)$$

$$\hat{C}_\alpha^{MN}(X_{N+1}) := \left\{ y \in \mathbb{R} : |y - \hat{y}_{N+1}| \leq \frac{1}{\hat{\sigma}(X_{N+1})} Q \left(1 - \alpha, w_{N+1} \delta_\infty + \sum_{i=1}^m w_{n+i} \delta_{R'_i} \right) \right\} \quad (23)$$

This potentially can make the PI more discriminative by modeling the heteroscedasticity explicitly.

As a reminder, all results shown in the main text are using $\hat{\mu}^{NN}$, with smoothing, and not normalized by MAD prediction (NN, Smooth, NM). Also, all choices will not break any theoretical guarantees, including Theorem 3.1 and 3.2.

The results are presented in Table 7 and 8, with the version shown in the main text boxed. All methods achieve target coverage rates as measured by MCR and TCR empirically. In general, we found that using \hat{y}^{KR} tends to give higher AUROC, with similar or lower MAD. It should be noted that the MAD prediction in “MN” requires a base classifier, which is \hat{y}^{NN} in our case. In other words, there is a mismatch in the “MN” version with \hat{y}^{KR} . We conjecture that if the MAD predictor is properly trained for \hat{y}^{KR} , the AUROC for this combination would be even higher (at no cost to other metrics). We also include the average width and count of finite PIs in Table 9 and 10. For most experiments

Table 7: MCR and TCR for different variants of LVD.

	\hat{y}^{KR}				\hat{y}^{NN}			
	No-smooth		Smooth		No-smooth		Smooth	
MCR	MN	base	MN	base	MN	base	MN	<i>base</i>
Yacht	96.6±4.5	97.4±2.0	95.2±4.6	95.5±2.3	96.1±4.9	97.9±1.7	94.7±5.0	96.8±2.2
Housing	96.8±3.4	97.1±2.8	96.0±3.9	95.7±3.5	97.3±2.2	97.8±2.1	96.1±2.6	96.2±2.9
Energy	92.8±2.7	92.4±2.9	92.5±2.6	92.4±2.9	94.0±1.7	94.1±1.6	93.9±1.7	94.0±1.6
Bike	91.6±1.2	93.8±0.8	91.6±1.2	94.1±0.8	90.6±0.5	90.5±0.8	90.4±0.6	90.4±0.8
Kin8nm	100.0±0.0	100.0±0.0	97.9±0.7	97.9±0.8	100.0±0.0	100.0±0.0	97.9±0.6	98.0±0.6
Concrete	99.6±0.7	99.6±0.8	96.7±2.3	97.0±1.1	99.7±0.6	99.6±0.7	97.0±2.1	97.4±1.3
QM8*	94.9±1.4	95.3±1.3	92.3±0.8	92.9±0.9	94.7±1.5	95.1±1.4	92.0±0.9	92.6±0.9
QM9*	94.0±1.7	94.1±1.6	90.6±0.4	90.4±0.5	93.5±1.5	93.7±1.5	90.3±0.4	90.3±0.6
TCR								
Yacht	96.9±4.0	96.9±5.4	93.1±7.6	94.6±5.2	95.4±7.4	99.2±2.4	93.8±7.1	98.5±3.2
Housing	95.7±4.2	96.2±4.4	93.3±9.3	91.4±8.3	98.1±3.3	97.1±4.0	98.1±2.5	96.2±4.4
Energy	86.8±6.2	83.5±9.7	85.8±6.1	83.2±10.2	88.1±4.8	87.1±5.9	87.7±4.8	86.8±5.8
Bike	91.8±1.0	91.9±2.1	90.9±1.6	91.6±2.7	92.0±1.3	90.8±1.5	91.6±1.3	90.2±1.7
Kin8nm	100.0±0.0	100.0±0.0	95.7±1.6	95.0±2.1	100.0±0.0	100.0±0.0	97.1±1.5	97.2±1.6
Concrete	99.0±2.1	99.3±1.6	93.9±4.5	94.4±3.6	99.5±1.0	99.5±1.5	96.8±3.8	97.1±3.4
QM8*	94.6±2.1	95.6±2.4	90.4±2.0	91.4±2.6	94.9±1.9	94.8±2.2	91.2±1.7	90.8±1.9
QM9*	94.4±4.4	94.3±4.5	88.5±3.7	88.0±3.7	94.9±3.1	94.8±3.4	90.1±2.3	89.7±2.5

Table 8: AUROC and MAD for different variants of LVD. Best AUROCs are in bold, and all are significantly higher than 50 (at $p = 0.05$). For MAD, the best for each task, if significantly better than the second-best (at $p = 0.05$), are in bold.

	\hat{y}^{KR}				\hat{y}^{NN}			
	No-smooth		Smooth		No-smooth		Smooth	
AUROC	MN	base	MN	base	MN	base	MN	<i>base</i>
Yacht	71.1±7.1	74.2±3.5	61.5±12.4	67.5±7.1	81.0±6.1	83.8±5.4	80.9±6.1	83.5±5.8
Housing	58.7±7.1	62.0±6.6	61.4±6.7	64.4±5.6	62.6±7.9	60.0±7.0	62.1±9.0	59.2±8.5
Energy	61.8±5.0	60.8±2.9	63.3±5.3	62.9±4.6	74.3±7.2	73.5±6.3	74.3±7.2	73.5±6.3
Bike	73.5±7.8	86.6±3.6	73.7±7.5	87.5±3.2	72.3±8.5	68.1±11.1	72.4±8.5	68.2±11.0
Kin8nm	55.7±1.8	55.9±2.1	60.5±1.9	61.8±1.6	57.1±2.4	56.8±2.4	61.6±1.6	60.3±1.1
Concrete	60.4±3.5	60.1±3.4	62.8±4.6	61.8±5.0	62.7±8.4	62.4±8.4	65.4±6.1	64.0±6.1
QM8*	73.2±9.6	72.8±11.9	75.9±9.0	75.2±11.9	72.9±7.7	71.3±9.5	74.1±6.9	71.3±9.4
QM9*	68.2±7.6	67.3±8.9	66.5±3.5	66.4±5.4	66.2±3.5	64.1±3.7	66.3±3.5	62.7±3.6
MAD								
Yacht	0.79±0.09	0.79±0.09	1.14±0.13	1.14±0.13	1.90±0.48	1.90±0.48	1.90±0.48	1.90±0.48
Housing	2.86±0.31	2.86±0.31	3.00±0.32	3.00±0.32	3.31±0.53	3.31±0.53	3.31±0.53	3.31±0.53
Energy	2.34±0.07	2.34±0.07	2.35±0.08	2.35±0.08	2.99±0.75	2.99±0.75	2.99±0.75	2.99±0.75
Bike	2.47±0.72	2.47±0.72	3.79±0.49	3.79±0.49	0.04±0.03	0.04±0.03	0.04±0.03	0.04±0.03
Kin8nm	0.06±0.00	0.06±0.00	0.07±0.00	0.07±0.00	0.07±0.00	0.07±0.00	0.07±0.00	0.07±0.00
Concrete	4.76±0.26	4.76±0.26	5.20±0.29	5.20±0.29	5.44±0.53	5.44±0.53	5.44±0.53	5.44±0.53
QM8*	0.01±0.01	0.01±0.01	0.01±0.01	0.01±0.01	0.01±0.01	0.01±0.01	0.01±0.01	0.01±0.01
QM9*	3.58±9.71	3.58±9.71	4.92±11.39	4.92±11.39	3.69±9.09	3.69±9.09	3.69±9.09	3.69±9.09

adding smoothness requirement and using \hat{y}^{KR} seems to achieve narrow PI, high AUROC, and low MAD. As noted earlier, training a separate model to model the residual of \hat{y}^{KR} might give additional discrimination (and possibly narrower PIs as well).

Table 9: Counts of finite PIs and average width for different variants of LVD (restricted to the subset for which all PIs are finite), with $\alpha = 0.5$. In the count table, the size of the test set is included in the parenthesis, and the lowest count (which is used for width computation) is underscored.

# finite @ 50%	\hat{g}^{KR}				\hat{g}^{NN}			
	No-smooth		Smooth		No-smooth		Smooth	
	MN	base	MN	base	MN	base	MN	<u>base</u>
Yacht(62)	60.7±1.9	60.7±1.9	61.9±0.3	61.9±0.3	60.7±1.9	60.7±1.9	61.9±0.3	61.9±0.3
Housing(101)	93.5±5.7	93.5±5.7	98.3±3.1	98.3±3.1	93.5±5.7	93.5±5.7	98.3±3.1	98.3±3.1
Energy(154)	154.0±0.0	154.0±0.0	154.0±0.0	154.0±0.0	154.0±0.0	154.0±0.0	154.0±0.0	154.0±0.0
Bike(3476)	3473.0±2.8	3473.0±2.8	3475.2±1.2	3475.2±1.2	3473.0±2.8	3473.0±2.8	3475.2±1.2	3475.2±1.2
Kin8nm(1638)	844.3±181.0	844.3±181.0	1610.1±10.2	1610.1±10.2	844.3±181.0	844.3±181.0	1610.1±10.2	1610.1±10.2
Concrete(206)	176.5±21.7	176.5±21.7	200.1±4.0	200.1±4.0	176.5±21.7	176.5±21.7	200.1±4.0	200.1±4.0
QM8*(4357)	4002.4±210.2	4002.4±210.2	4317.3±22.9	4317.3±22.9	4002.4±210.2	4002.4±210.2	4317.3±22.9	4317.3±22.9
QM9*(26744)	25376.7±792.3	25376.7±792.3	26616.7±39.8	26616.7±39.8	25376.7±792.3	25376.7±792.3	26616.7±39.8	26616.7±39.8
Width @ 50%								
Yacht	1.8±0.5	1.7±0.5	2.2±0.5	2.1±0.4	4.5±0.9	4.4±0.9	4.1±0.9	3.8±0.9
Housing	5.9±0.6	5.7±0.8	5.5±0.6	5.3±0.7	7.2±1.1	7.0±1.1	6.7±1.3	6.4±1.0
Energy	4.3±0.5	4.3±0.3	4.3±0.4	4.3±0.3	6.2±1.5	6.1±1.4	6.2±1.5	6.1±1.4
Bike	5.4±1.5	4.8±1.3	8.3±1.4	7.3±0.9	0.1±0.1	0.1±0.0	0.1±0.1	0.1±0.0
Kin8nm	0.2±0.0	0.2±0.0	0.1±0.0	0.1±0.0	0.2±0.0	0.2±0.0	0.1±0.0	0.1±0.0
Concrete	11.5±1.2	11.2±1.1	10.1±1.1	9.8±1.1	13.1±2.1	12.8±2.2	10.8±1.8	10.5±1.8
QM8*	0.0±0.0	0.0±0.0	0.0±0.0	0.0±0.0	0.0±0.0	0.0±0.0	0.0±0.0	0.0±0.0
QM9*	6.1±17.3	5.5±15.6	7.6±18.6	6.8±16.7	6.3±15.8	5.6±14.2	5.7±14.7	5.0±12.9

Table 10: Same as Table 9, but with $\alpha = 0.1$.

# finite @ 90%	\hat{g}^{KR}				\hat{g}^{NN}			
	No-smooth		Smooth		No-smooth		Smooth	
	MN	base	MN	base	MN	base	MN	<u>base</u>
Yacht(62)	35.1±5.8	35.1±5.8	40.9±2.8	40.9±2.8	35.1±5.8	35.1±5.8	40.9±2.8	40.9±2.8
Housing(101)	54.5±22.1	54.5±22.1	69.0±19.1	69.0±19.1	54.5±22.1	54.5±22.1	69.0±19.1	69.0±19.1
Energy(154)	145.1±11.0	145.1±11.0	145.1±11.0	145.1±11.0	145.1±11.0	145.1±11.0	145.1±11.0	145.1±11.0
Bike(3476)	3458.5±11.4	3458.5±11.4	3467.5±4.4	3467.5±4.4	3458.5±11.4	3458.5±11.4	3467.5±4.4	3467.5±4.4
Kin8nm(1638)	0.4±1.0	0.4±1.0	938.0±123.7	938.0±123.7	0.4±1.0	0.4±1.0	938.0±123.7	938.0±123.7
Concrete(206)	28.8±24.8	28.8±24.8	133.8±20.1	133.8±20.1	28.8±24.8	28.8±24.8	133.8±20.1	133.8±20.1
QM8*(4357)	2936.9±587.9	2936.9±587.9	4041.6±136.8	4041.6±136.8	2936.9±587.9	2936.9±587.9	4041.6±136.8	4041.6±136.8
QM9*(26744)	21347.5±2850.8	21347.5±2850.8	26147.0±151.6	26147.0±151.6	21347.5±2850.8	21347.5±2850.8	26147.0±151.6	26147.0±151.6
Width @ 90%								
Yacht	5.69±2.98	2.21±0.58	7.68±5.57	2.33±0.41	5.82±3.29	3.03±1.40	4.85±2.08	2.97±1.41
Housing	32.33±34.63	14.14±2.09	22.67±21.69	13.29±1.85	43.46±56.19	15.50±2.89	25.76±20.69	14.48±2.64
Energy	14.61±7.54	12.47±1.48	15.07±8.52	12.49±1.47	15.94±10.07	12.91±2.03	15.92±10.08	12.89±2.02
Bike	21.46±11.96	8.33±2.43	35.62±21.29	11.78±1.72	0.19±0.11	0.15±0.13	0.19±0.12	0.15±0.13
Kin8nm	0.44±0.03	0.36±0.02	0.27±0.12	0.25±0.03	0.39±0.08	0.37±0.02	0.25±0.11	0.24±0.02
Concrete	27.25±4.77	26.30±4.71	20.55±4.06	21.76±2.67	28.79±6.79	28.25±5.16	21.56±4.00	23.41±3.50
QM8*	0.05±0.03	0.04±0.02	0.04±0.02	0.04±0.02	0.05±0.03	0.04±0.02	0.04±0.02	0.04±0.02
QM9*	14.87±41.31	15.01±42.57	17.86±43.59	17.20±43.19	14.84±38.27	15.22±40.44	13.65±35.71	14.04±37.44

B.4 Additional Results on QM8/QM9 sub-tasks

Table 12 and 11 show the metrics for validity and discrimination, respectively, of different variants of LVD, and the two valid baselines. Table 13 shows the number of widths of PIs by different methods on the QM subtasks. Table 14 shows the coverage rates for a list of functional groups from the OPENSMILES project⁸. We keep only the subset of data whose original SMILES representation contains the corresponding functional group’s SMILES representation, and compute the average coverage rate for each of the twelve targets of QM9 dataset⁹. If LVD is actually conditionally valid, then the conditional coverage rate should not be significantly lower than the target (90%). Again, it is worth noting that LVD is only *approximately* conditionally valid, and the raw SMILES functional groups were not used anywhere in the entire pipeline. However, LVD is still almost always valid empirically.

⁸<http://opensmiles.org/opensmiles.html>

⁹We only did this for QM9 because the size of QM8 is not enough for this task.

Table 11: AUROC and MAD for QM8 and QM9 sub-tasks. The best AUROCs are in bold, and AUROCs **not** significantly higher than 50 at $p = 0.05$ are underscored. For MAD, the best MADs, if significantly better than the second baseline at $p = 0.05$, are in bold.

AUROC	LVD								Conformal Baselines	
	\hat{y}^{KR}				\hat{y}^{NN}					
	No-smooth		Smooth		No-smooth		Smooth			
	MN	base	MN	base	MN	base	MN	<u>base</u>	MADSplit	CQR
QM8(E1-CC2)	64.3±1.4	61.8±1.5	67.9±0.9	64.9±1.0	66.2±1.0	63.2±1.2	68.2±0.9	62.9±1.4	67.7±0.8	57.9±3.8
QM8(E2-CC2)	62.5±1.5	60.2±1.3	66.7±0.8	63.2±1.2	64.3±1.2	61.1±1.2	66.8±1.1	61.7±1.2	66.2±1.0	56.8±3.9
QM8(f1-CC2)	83.8±2.1	85.7±2.5	85.7±1.0	87.9±0.8	80.2±1.0	80.5±1.2	80.5±1.2	80.1±1.4	80.0±1.0	70.5±2.9
QM8(f2-CC2)	81.4±2.6	82.9±2.2	84.3±1.3	86.0±0.7	81.7±1.0	82.1±0.7	82.1±0.8	82.3±0.5	80.9±1.1	78.5±5.7
QM8(E1-PBE0)	64.7±1.6	61.8±1.6	67.6±0.8	63.9±1.6	66.2±1.1	62.6±1.1	68.3±0.9	62.6±1.1	67.6±0.9	55.2±5.0
QM8(E2-PBE0)	63.9±1.4	60.2±1.2	66.0±1.0	61.8±1.2	65.1±1.3	61.3±1.4	66.6±1.2	61.2±1.5	66.3±1.2	55.9±2.2
QM8(f1-PBE0)	83.8±2.2	86.0±2.0	85.2±1.4	87.8±0.7	79.0±1.1	78.8±1.0	79.1±1.1	78.1±1.7	79.0±1.0	67.2±2.7
QM8(f2-PBE0)	80.1±2.3	82.1±2.8	82.8±1.1	85.2±0.9	80.8±0.9	81.0±0.8	81.2±1.2	81.1±1.1	80.3±1.0	79.9±3.1
QM8(E1-PBE0.1)	64.8±1.6	61.8±1.6	67.6±0.9	63.9±1.6	66.3±1.4	62.6±1.1	68.2±0.7	62.4±0.8	67.4±0.8	56.9±2.5
QM8(E2-PBE0.1)	63.8±1.4	60.2±1.2	65.8±1.0	61.8±1.2	64.6±1.3	60.8±1.5	66.1±0.9	60.8±1.5	66.0±1.1	55.2±2.3
QM8(f1-PBE0.1)	83.8±2.2	86.0±2.0	85.1±1.4	87.8±0.7	79.5±1.5	79.3±1.2	79.7±1.4	78.7±1.8	79.4±1.3	68.1±3.8
QM8(f2-PBE0.1)	80.1±2.3	82.1±2.8	82.9±1.1	85.2±0.9	81.1±0.7	81.3±0.8	81.6±1.0	81.4±1.1	80.6±0.9	76.7±6.9
QM8(E1-CAM)	63.4±1.6	61.4±1.2	67.7±1.1	64.8±1.0	65.4±1.2	62.2±1.0	68.2±1.0	63.2±0.7	67.4±1.0	58.0±3.9
QM8(E2-CAM)	63.9±2.2	61.2±1.7	66.6±0.8	63.3±1.8	65.1±2.1	61.7±1.6	66.9±1.4	62.4±2.1	66.5±1.5	56.8±3.3
QM8(f1-CAM)	85.8±1.5	87.7±1.5	87.2±1.0	89.5±0.5	78.7±1.2	79.2±1.2	78.7±1.3	78.8±1.2	78.4±1.2	73.1±2.0
QM8(f2-CAM)	81.5±2.1	83.0±2.2	84.8±1.0	86.8±0.8	82.7±1.1	82.9±1.0	83.2±1.0	83.3±1.1	82.1±1.0	81.4±2.3
QM9(mu)	71.7±0.6	67.6±0.5	71.8±1.0	66.6±1.7	72.6±1.1	68.2±0.5	73.9±0.7	68.0±1.1	73.7±0.7	57.4±3.4
QM9(alpha)	61.6±1.2	60.3±1.3	66.2±1.3	65.9±1.9	65.3±0.8	63.2±0.9	65.3±0.6	61.3±1.4	64.0±0.5	45.9±7.7
QM9(homo)	61.2±0.9	58.3±0.5	61.9±0.5	58.4±0.8	62.2±0.4	58.6±0.5	62.9±0.3	58.1±0.9	62.6±0.4	<u>38.7±20.8</u>
QM9(lumo)	60.6±0.7	58.6±0.7	61.5±0.7	59.3±0.7	61.2±0.8	58.5±0.4	62.4±0.4	58.1±0.4	62.2±0.4	<u>58.4±20.1</u>
QM9(gap)	62.3±1.0	60.4±1.0	62.8±0.5	60.5±0.8	62.8±0.9	60.1±0.7	63.5±0.5	59.6±0.6	63.1±0.5	<u>60.2±25.0</u>
QM9(r2)	67.8±1.1	64.1±1.1	68.5±1.2	65.0±1.0	69.3±0.7	64.7±0.6	69.8±0.5	63.1±0.9	69.5±0.5	63.8±0.9
QM9(zpve)	60.5±1.7	60.7±1.7	65.4±0.9	65.6±1.4	62.7±0.5	61.8±0.7	61.3±0.3	58.8±0.6	60.4±0.4	67.5±19.1
QM9(u0)	77.6±3.4	79.2±2.7	68.9±2.4	72.9±1.6	68.3±0.5	67.7±0.4	67.8±0.6	66.1±1.0	64.6±0.9	54.9±2.0
QM9(u298)	77.6±3.3	79.1±2.6	68.8±2.5	72.9±1.7	68.4±0.6	67.9±0.6	67.9±0.8	66.0±1.2	64.7±1.0	55.8±2.2
QM9(h298)	77.5±3.2	79.1±2.6	68.9±2.5	72.9±1.6	68.4±0.7	67.9±0.7	67.9±0.8	66.2±1.2	64.7±0.9	55.7±2.0
QM9(g298)	77.6±3.3	79.2±2.7	68.9±2.4	72.9±1.7	68.6±0.7	68.0±0.7	68.0±0.8	66.1±1.1	64.8±0.9	54.5±1.8
QM9(cv)	62.6±1.0	60.8±0.9	65.0±1.1	64.0±0.9	64.6±1.1	62.3±0.8	65.3±0.7	60.9±0.8	64.6±0.7	<u>47.5±9.1</u>
MAD										
QM8(E1-CC2)	0.01±0.00	0.01±0.00	0.01±0.00	0.01±0.00	0.01±0.00	0.01±0.00	0.01±0.00	0.01±0.00	0.01±0.00	0.02±0.00
QM8(E2-CC2)	0.01±0.00	0.01±0.00	0.01±0.00	0.01±0.00	0.01±0.00	0.01±0.00	0.01±0.00	0.01±0.00	0.01±0.00	0.02±0.00
QM8(f1-CC2)	0.01±0.00	0.01±0.00	0.01±0.00	0.01±0.00	0.01±0.00	0.01±0.00	0.01±0.00	0.01±0.00	0.01±0.00	0.03±0.00
QM8(f2-CC2)	0.03±0.00	0.03±0.00	0.03±0.00	0.03±0.00	0.03±0.00	0.03±0.00	0.03±0.00	0.03±0.00	0.03±0.00	0.06±0.01
QM8(E1-PBE0)	0.01±0.00	0.01±0.00	0.01±0.00	0.01±0.00	0.01±0.00	0.01±0.00	0.01±0.00	0.01±0.00	0.01±0.00	0.02±0.00
QM8(E2-PBE0)	0.01±0.00	0.01±0.00	0.01±0.00	0.01±0.00	0.01±0.00	0.01±0.00	0.01±0.00	0.01±0.00	0.01±0.00	0.02±0.00
QM8(f1-PBE0)	0.01±0.00	0.01±0.00	0.01±0.00	0.01±0.00	0.01±0.00	0.01±0.00	0.01±0.00	0.01±0.00	0.01±0.00	0.03±0.00
QM8(f2-PBE0)	0.02±0.00	0.02±0.00	0.02±0.00	0.02±0.00	0.02±0.00	0.02±0.00	0.02±0.00	0.02±0.00	0.02±0.00	0.05±0.01
QM8(E1-PBE0.1)	0.01±0.00	0.01±0.00	0.01±0.00	0.01±0.00	0.01±0.00	0.01±0.00	0.01±0.00	0.01±0.00	0.01±0.00	0.02±0.00
QM8(E2-PBE0.1)	0.01±0.00	0.01±0.00	0.01±0.00	0.01±0.00	0.01±0.00	0.01±0.00	0.01±0.00	0.01±0.00	0.01±0.00	0.02±0.00
QM8(f1-PBE0.1)	0.01±0.00	0.01±0.00	0.01±0.00	0.01±0.00	0.01±0.00	0.01±0.00	0.01±0.00	0.01±0.00	0.01±0.00	0.03±0.01
QM8(f2-PBE0.1)	0.02±0.00	0.02±0.00	0.02±0.00	0.02±0.00	0.02±0.00	0.02±0.00	0.02±0.00	0.02±0.00	0.02±0.00	0.05±0.01
QM8(E1-CAM)	0.01±0.00	0.01±0.00	0.01±0.00	0.01±0.00	0.01±0.00	0.01±0.00	0.01±0.00	0.01±0.00	0.01±0.00	0.02±0.01
QM8(E2-CAM)	0.01±0.00	0.01±0.00	0.01±0.00	0.01±0.00	0.01±0.00	0.01±0.00	0.01±0.00	0.01±0.00	0.01±0.00	0.02±0.00
QM8(f1-CAM)	0.01±0.00	0.01±0.00	0.01±0.00	0.01±0.00	0.01±0.00	0.01±0.00	0.01±0.00	0.01±0.00	0.01±0.00	0.04±0.01
QM8(f2-CAM)	0.02±0.00	0.02±0.00	0.02±0.00	0.02±0.00	0.02±0.00	0.02±0.00	0.02±0.00	0.02±0.00	0.02±0.00	0.05±0.01
QM9(mu)	0.49±0.01	0.49±0.01	0.51±0.01	0.51±0.01	0.48±0.00	0.48±0.00	0.48±0.00	0.48±0.00	0.48±0.00	2.01±1.24
QM9(alpha)	0.69±0.03	0.69±0.03	1.10±0.07	1.10±0.07	0.70±0.01	0.70±0.01	0.70±0.01	0.70±0.01	0.70±0.01	9.79±0.83
QM9(homo)	0.00±0.00	0.00±0.00	0.00±0.00	0.00±0.00	0.00±0.00	0.00±0.00	0.00±0.00	0.00±0.00	0.00±0.00	2.13±2.01
QM9(lumo)	0.00±0.00	0.00±0.00	0.01±0.00	0.01±0.00	0.00±0.00	0.00±0.00	0.00±0.00	0.00±0.00	0.00±0.00	5.65±3.33
QM9(gap)	0.01±0.00	0.01±0.00	0.01±0.00	0.01±0.00	0.01±0.00	0.01±0.00	0.01±0.00	0.01±0.00	0.01±0.00	4.34±3.35
QM9(r2)	35.56±1.29	35.56±1.29	42.12±1.56	42.12±1.56	33.53±0.36	33.53±0.36	33.53±0.36	33.53±0.36	33.53±0.36	188.64±9.50
QM9(zpve)	0.00±0.00	0.00±0.00	0.00±0.00	0.00±0.00	0.00±0.00	0.00±0.00	0.00±0.00	0.00±0.00	0.00±0.00	4.42±3.93
QM9(u0)	1.46±0.18	1.46±0.18	3.69±0.33	3.69±0.33	2.29±0.07	2.29±0.07	2.29±0.07	2.29±0.07	2.29±0.07	40.85±3.49
QM9(u298)	1.46±0.18	1.46±0.18	3.69±0.33	3.69±0.33	2.29±0.06	2.29±0.06	2.29±0.06	2.29±0.06	2.29±0.06	40.64±3.81
QM9(h298)	1.45±0.18	1.45±0.18	3.69±0.33	3.69±0.33	2.29±0.06	2.29±0.06	2.29±0.06	2.29±0.06	2.29±0.06	40.84±3.03
QM9(g298)	1.46±0.18	1.46±0.18	3.70±0.33	3.70±0.33	2.29±0.07	2.29±0.07	2.29±0.07	2.29±0.07	2.29±0.07	41.02±3.81
QM9(cv)	0.34±0.01	0.34±0.01	0.47±0.02	0.47±0.02	0.33±0.01	0.33±0.01	0.33±0.01	0.33±0.01	0.33±0.01	5.03±1.55

Table 12: MCR and TCR for QM8 and QM9, for 90% PI. Numbers *not* significantly lower than 90% are in bold. Like in the main text, MADSplit and CQR achieves 90% marginal coverage rate empirically as expected, but fail to cover data with more extreme responses (in the tails). Variants of LVD almost always cover empirically, measured by both MCR and TCR.

MCR	LVD								Conformal Baselines	
	\hat{y}^{KR}				\hat{y}^{NN}				MADSplit	CQR
	No-smooth		Smooth		No-smooth		Smooth			
	MN	base	MN	base	MN	base	MN	base		
QM8(E1-CC2)	96.3±0.7	96.3±0.8	92.6±0.9	92.7±0.6	96.2±0.8	96.2±0.6	92.3±0.6	92.5±0.5	90.0±0.5	90.1±0.7
QM8(E2-CC2)	96.2±1.0	96.2±0.8	92.0±0.5	92.2±0.7	96.1±1.0	96.2±0.7	92.0±0.5	92.2±0.5	89.8±0.6	90.1±0.5
QM8(f1-CC2)	93.9±0.9	94.8±0.9	92.3±0.7	93.8±0.8	93.7±1.0	94.0±1.2	92.2±0.8	92.5±1.1	90.1±0.7	90.2±0.7
QM8(f2-CC2)	94.8±1.3	95.1±1.1	93.0±0.6	93.6±0.6	94.3±1.3	95.1±1.3	92.5±0.8	93.6±0.6	89.9±0.7	89.9±0.7
QM8(E1-PBE0)	95.9±0.5	96.0±0.6	92.3±0.7	92.7±0.6	95.7±0.7	95.9±0.6	91.9±0.8	92.5±0.6	89.7±0.5	90.2±0.5
QM8(E2-PBE0)	95.0±0.9	95.4±0.9	91.8±0.5	92.4±0.8	95.0±0.9	95.3±0.9	91.7±0.6	92.3±0.6	90.0±0.5	90.0±0.6
QM8(f1-PBE0)	93.7±1.1	94.3±1.2	92.4±1.0	93.1±1.0	93.4±1.2	93.9±1.4	91.8±1.3	92.4±1.2	90.3±0.8	90.2±0.9
QM8(f2-PBE0)	94.0±1.8	94.6±1.8	91.9±1.1	92.5±0.9	93.9±1.9	94.8±1.6	91.6±1.2	92.8±0.9	89.9±0.9	89.7±0.5
QM8(E1-PBE0.1)	95.8±0.6	96.0±0.6	92.2±0.6	92.7±0.6	95.6±0.7	95.9±0.5	91.9±0.8	92.5±0.7	89.8±0.5	89.8±0.6
QM8(E2-PBE0.1)	94.9±0.8	95.4±0.9	91.7±0.4	92.4±0.8	95.0±1.0	95.3±0.9	91.8±0.5	92.3±0.6	90.2±0.5	90.0±0.4
QM8(f1-PBE0.1)	93.6±1.0	94.3±1.2	92.3±0.9	93.1±1.0	93.1±1.4	93.9±1.3	91.6±1.3	92.3±1.4	89.9±1.0	90.0±0.4
QM8(f2-PBE0.1)	94.2±1.8	94.6±1.8	92.0±1.1	92.5±0.9	94.0±1.9	94.8±1.7	91.8±1.1	92.8±0.9	89.9±0.7	89.7±0.8
QM8(E1-CAM)	96.3±1.1	96.5±0.9	92.7±0.9	93.2±0.8	96.2±1.2	96.4±0.9	92.3±0.8	92.8±0.6	89.9±0.5	90.2±0.4
QM8(E2-CAM)	95.3±1.0	95.6±1.1	92.1±0.7	92.6±0.8	95.4±0.8	95.6±0.9	92.1±0.5	92.5±0.7	90.0±0.5	90.0±0.6
QM8(f1-CAM)	93.7±1.0	94.7±1.2	92.2±0.6	93.5±0.8	93.3±0.9	93.8±1.2	91.7±0.6	92.2±0.7	89.8±0.7	89.9±0.7
QM8(f2-CAM)	94.7±1.1	95.0±0.8	92.7±0.7	93.4±0.6	94.5±1.1	95.2±0.9	92.5±0.7	93.5±0.7	90.0±0.9	90.3±0.8
QM9(mu)	92.5±1.7	93.2±1.6	90.4±0.4	91.3±0.5	92.6±1.7	93.3±1.5	90.6±0.4	91.4±0.4	90.1±0.2	90.0±0.3
QM9(alpha)	94.7±1.5	94.6±1.6	90.5±0.4	89.7±0.4	94.5±1.5	94.6±1.6	90.1±0.3	89.7±0.4	90.0±0.2	89.9±0.2
QM9(homo)	92.3±0.6	92.5±0.7	90.4±0.4	90.4±0.2	92.4±0.6	92.6±0.7	90.6±0.3	90.7±0.3	90.0±0.3	89.9±0.3
QM9(lumo)	93.5±0.9	93.5±1.0	90.5±0.3	90.4±0.3	93.5±0.9	93.6±0.9	90.7±0.4	90.6±0.3	90.1±0.3	89.9±0.4
QM9(gap)	93.0±1.2	93.1±1.2	90.5±0.3	90.4±0.2	93.0±1.1	93.2±1.1	90.6±0.3	90.7±0.3	90.1±0.2	89.9±0.3
QM9(r2)	92.6±1.1	93.0±1.2	90.1±0.3	90.5±0.3	92.6±1.2	93.1±1.1	90.4±0.4	90.8±0.5	89.9±0.4	90.1±0.3
QM9(zpve)	95.3±1.2	95.4±1.2	90.5±0.1	90.1±0.3	95.2±1.3	95.3±1.4	90.3±0.2	89.9±0.2	90.0±0.2	90.0±0.2
QM9(u0)	94.9±1.5	94.8±1.6	90.9±0.5	90.6±0.5	93.3±1.3	93.4±1.3	90.1±0.2	90.0±0.3	89.9±0.2	90.1±0.2
QM9(u298)	95.1±1.8	95.0±1.9	90.9±0.5	90.6±0.5	93.6±1.7	93.7±1.8	90.0±0.2	89.9±0.3	89.9±0.2	90.1±0.2
QM9(h298)	95.0±1.6	94.9±1.7	90.9±0.5	90.6±0.5	93.5±1.4	93.6±1.4	90.1±0.2	90.0±0.3	89.9±0.2	90.1±0.2
QM9(g298)	94.9±1.5	94.8±1.6	90.8±0.5	90.6±0.5	93.3±1.4	93.4±1.3	90.0±0.2	89.9±0.3	89.9±0.2	90.1±0.2
QM9(cv)	94.3±1.4	94.4±1.5	90.4±0.3	89.9±0.5	94.2±1.5	94.4±1.5	90.4±0.4	90.1±0.4	90.0±0.2	90.0±0.4
TCR										
QM8(E1-CC2)	94.4±1.2	94.3±1.4	89.6±1.9	89.3±0.9	95.2±0.9	94.3±1.5	91.3±1.2	90.2±1.3	88.1±1.5	83.5±6.4
QM8(E2-CC2)	95.5±1.5	94.9±1.7	89.6±1.2	88.6±1.4	95.8±1.6	95.6±1.5	90.7±1.7	90.1±1.7	87.4±2.2	84.4±4.4
QM8(f1-CC2)	94.5±2.2	97.0±1.7	90.4±1.5	93.6±1.4	94.9±1.3	94.1±2.0	91.4±1.2	90.5±1.8	85.0±1.8	80.1±2.8
QM8(f2-CC2)	95.6±2.5	96.2±2.7	91.8±1.6	92.3±1.7	95.7±2.6	95.2±2.9	92.4±1.6	91.4±1.5	84.9±2.1	73.3±4.8
QM8(E1-PBE0)	94.0±1.4	94.2±1.2	89.9±1.8	89.9±1.5	94.4±0.8	94.2±1.5	90.9±1.2	90.3±1.5	87.8±1.8	80.9±4.6
QM8(E2-PBE0)	94.1±1.6	93.8±2.0	90.0±1.6	89.7±2.0	94.8±1.4	94.2±1.9	90.9±1.7	90.5±2.0	87.5±1.8	82.1±5.8
QM8(f1-PBE0)	94.3±2.3	97.3±1.5	90.9±3.0	94.4±1.8	94.5±2.0	95.2±1.9	91.1±2.7	91.8±2.1	85.1±1.9	80.4±2.5
QM8(f2-PBE0)	94.5±3.4	95.6±3.4	90.1±2.4	90.9±1.5	95.1±3.2	95.1±3.6	90.9±2.4	90.2±1.8	84.4±2.6	74.6±6.2
QM8(E1-PBE0.1)	94.0±1.3	94.2±1.2	89.8±1.5	89.9±1.5	94.3±1.2	93.9±1.6	90.7±1.4	90.3±1.9	87.8±2.0	83.4±4.4
QM8(E2-PBE0.1)	94.2±1.4	93.8±2.0	90.1±1.6	89.7±2.0	94.9±1.5	94.3±2.1	91.0±1.5	90.4±2.2	87.9±1.8	82.0±5.5
QM8(f1-PBE0.1)	94.2±2.3	97.3±1.5	90.7±2.8	94.4±1.8	93.9±2.1	95.2±1.8	90.6±2.7	91.7±2.5	84.1±2.0	81.1±2.4
QM8(f2-PBE0.1)	94.7±3.2	95.6±3.4	90.0±2.1	90.9±1.5	95.0±3.2	95.0±3.7	90.8±2.3	90.3±1.9	84.2±2.4	73.3±3.8
QM8(E1-CAM)	94.0±1.7	94.1±1.7	89.1±2.4	90.0±1.3	94.3±1.5	93.8±1.9	90.2±1.4	89.8±1.7	86.5±1.4	81.4±5.8
QM8(E2-CAM)	95.1±1.4	95.0±1.8	90.7±1.2	90.4±1.5	95.4±1.4	95.4±1.9	91.8±1.0	91.1±1.5	88.1±1.7	83.5±5.0
QM8(f1-CAM)	95.3±2.3	98.8±1.2	92.1±1.4	96.2±0.7	95.1±1.6	95.9±1.4	92.3±0.8	93.0±1.3	86.7±1.1	81.9±3.3
QM8(f2-CAM)	95.7±1.7	96.8±1.8	91.5±0.9	92.8±0.9	95.9±1.7	96.0±1.9	91.7±1.5	91.2±1.5	85.0±2.0	73.5±4.6
QM9(mu)	83.2±4.7	82.9±4.6	77.4±1.5	77.1±1.7	87.0±3.5	86.0±3.4	83.1±1.5	81.9±1.1	79.8±1.5	64.7±4.2
QM9(alpha)	96.7±1.3	96.7±1.5	88.9±0.7	87.9±0.7	97.4±1.1	97.5±1.2	90.7±0.9	90.3±0.9	87.3±0.8	69.9±2.3
QM9(homo)	91.7±1.4	91.4±1.5	87.2±0.8	86.7±1.0	93.0±1.0	92.9±0.9	89.7±0.7	89.4±1.0	86.5±0.5	89.8±2.7
QM9(lumo)	93.4±1.3	93.5±1.2	88.2±0.8	88.1±0.7	94.7±0.7	94.7±0.8	91.1±0.9	90.7±1.0	89.7±0.9	87.5±1.9
QM9(gap)	92.0±1.8	91.9±2.0	87.6±0.6	86.9±0.9	93.7±1.4	93.6±1.5	90.3±0.8	90.0±1.0	87.9±0.8	88.1±1.3
QM9(r2)	94.1±2.1	93.7±2.0	88.2±0.8	88.0±1.2	95.3±1.7	95.0±1.7	90.9±0.7	90.6±1.2	87.6±0.8	67.0±4.3
QM9(zpve)	97.0±1.0	97.1±0.9	90.4±0.7	90.1±0.7	96.7±1.2	96.9±1.2	91.2±0.9	90.9±0.8	90.5±0.6	88.3±4.5
QM9(u0)	97.3±1.5	97.2±1.6	91.2±0.9	90.7±0.9	95.9±1.5	96.1±1.7	90.7±0.5	90.4±0.8	84.1±1.0	80.1±3.2
QM9(u298)	97.4±1.7	97.4±1.8	91.2±0.8	90.7±0.9	96.2±1.8	96.2±1.9	90.6±0.4	90.4±0.8	84.0±0.9	79.8±3.3
QM9(h298)	97.4±1.7	97.3±1.7	91.2±0.8	90.7±0.9	96.1±1.8	96.1±1.9	90.7±0.4	90.4±0.7	84.0±1.1	80.3±2.9
QM9(g298)	97.3±1.6	97.2±1.7	91.1±0.7	90.7±0.9	96.0±1.6	96.0±1.7	90.7±0.4	90.3±0.7	84.0±1.1	80.0±2.3
QM9(cv)	95.9±1.8	95.9±2.0	89.2±0.7	88.2±1.0	96.5±1.5	96.6±1.5	91.0±0.7	90.8±0.7	87.8±0.6	80.4±7.7

Table 13: Average width for 50% and 90% PIs of different methods. Narrowest PIs are in bold, and further underscored if significantly narrower than the second best (at $p = 0.05$). As a reminder, there are 4357 data in QM8's test set and 26744 in QM9's. Among these valid methods, LVD's 50% PIs are the narrowest, and still competitive at 90% despite satisfying a stronger coverage requirement.

Width @ 50%	# finite	$\hat{y}^{K,R}$				LVD				$\hat{y}^{N,N}$				Conformal Baselines			
		No-smooth		Smooth		No-smooth		Smooth		No-smooth		Smooth		MADsplit		base	
		base	mn	base	mn	base	mn	base	mn	base	mn	base	mn	base	mn	base	mn
QM8(EI-CC2)	3791.5±189.4	1.2e-02±2.1e-04	1.1e-02±3.0e-04	1.1e-02±6.0e-04	9.8e-03±5.0e-04	1.3e-02±5.0e-04	1.3e-02±5.0e-04	1.2e-02±4.0e-04	1.1e-02±5.0e-04	1.2e-02±4.0e-04	1.1e-02±5.0e-04	9.6e-03±4.0e-04	1.0e-02±4.0e-04	1.0e-02±4.0e-04	3.2e-02±4.1e-03	1.2e-02±4.0e-04	3.2e-02±4.1e-03
QM8(E2-CC2)	3829.8±126.6	1.4e-02±1.6e-03	1.3e-02±5.0e-04	1.3e-02±4.0e-04	1.6e-02±1.6e-03	1.4e-02±4.0e-04	1.5e-02±9.0e-04	1.4e-02±7.0e-04	1.2e-02±3.0e-04	1.4e-02±7.0e-04	1.2e-02±3.0e-04	1.1e-02±2.1e-03	1.1e-02±2.1e-03	1.1e-02±2.1e-03	2.8e-02±3.3e-03	1.2e-02±3.0e-04	2.8e-02±3.3e-03
QM8(R1-CC2)	4066.0±231.7	2.1e-02±1.6e-03	1.9e-02±1.2e-03	1.8e-02±2.1e-03	4.6e-02±2.5e-03	4.1e-02±2.1e-03	4.5e-02±3.2e-03	4.9e-02±3.2e-03	4.7e-02±5.1e-03	4.6e-02±3.2e-03	4.7e-02±5.1e-03	4.2e-02±4.7e-03	4.2e-02±4.7e-03	4.2e-02±4.7e-03	3.7e-02±5.1e-02	4.1e-02±3.2e-03	3.7e-02±5.1e-02
QM8(E1-PBE0.1)	3932.1±133.8	1.2e-02±3.0e-04	1.1e-02±2.0e-04	1.1e-02±6.0e-04	1.1e-02±3.0e-04	9.6e-03±3.0e-04	1.3e-02±5.0e-04	1.2e-02±4.0e-04	1.1e-02±3.0e-04	1.2e-02±4.0e-04	1.1e-02±3.0e-04	1.1e-02±3.0e-04	1.1e-02±3.0e-04	1.1e-02±3.0e-04	2.9e-02±7.9e-03	1.2e-02±3.0e-04	2.9e-02±7.9e-03
QM8(E2-PBE0)	4063.2±133.4	1.3e-02±4.0e-04	1.2e-02±3.0e-04	1.2e-02±6.0e-04	1.1e-02±3.0e-04	1.3e-02±5.0e-04	1.3e-02±5.0e-04	1.2e-02±4.0e-04	1.1e-02±3.0e-04	1.2e-02±4.0e-04	1.1e-02±3.0e-04	1.1e-02±3.0e-04	1.1e-02±3.0e-04	1.1e-02±3.0e-04	3.4e-02±9.1e-03	1.2e-02±3.0e-04	3.4e-02±9.1e-03
QM8(R1-PBE0)	4152.1±159.3	1.8e-02±9.0e-04	1.5e-02±9.0e-04	1.6e-02±2.0e-03	1.4e-02±2.0e-03	1.4e-02±2.0e-03	2.0e-02±1.0e-03	1.7e-02±1.0e-03	1.6e-02±2.3e-03	1.6e-02±2.3e-03	1.6e-02±2.3e-03	1.4e-02±2.0e-03	1.4e-02±2.0e-03	1.4e-02±2.0e-03	3.2e-02±5.9e-03	1.4e-02±2.0e-03	3.2e-02±5.9e-03
QM8(R2-PBE0)	4059.8±240.7	3.9e-02±1.0e-03	3.4e-02±1.0e-03	3.4e-02±3.5e-03	1.4e-02±2.9e-03	1.4e-02±2.9e-03	4.1e-02±1.6e-03	3.6e-02±1.7e-03	3.4e-02±3.5e-03	3.4e-02±3.5e-03	3.4e-02±3.5e-03	3.0e-02±2.8e-03	3.0e-02±2.8e-03	3.0e-02±2.8e-03	4.2e-02±5.9e-03	3.0e-02±2.8e-03	4.2e-02±5.9e-03
QM8(E1-PBE0.1)	3932.1±133.8	1.2e-02±2.0e-04	1.1e-02±2.0e-04	1.1e-02±4.0e-04	9.6e-03±3.0e-04	1.3e-02±5.0e-04	1.3e-02±5.0e-04	1.1e-02±4.0e-04	1.1e-02±4.0e-04	1.1e-02±4.0e-04	1.1e-02±4.0e-04	9.6e-03±3.0e-04	1.1e-02±4.0e-04	1.1e-02±4.0e-04	3.1e-02±4.8e-03	1.1e-02±4.0e-04	3.1e-02±4.8e-03
QM8(E2-PBE0.1)	4063.2±133.4	1.3e-02±4.0e-04	1.2e-02±3.0e-04	1.2e-02±6.0e-04	1.1e-02±3.0e-04	1.3e-02±5.0e-04	1.3e-02±5.0e-04	1.2e-02±4.0e-04	1.1e-02±3.0e-04	1.2e-02±4.0e-04	1.1e-02±3.0e-04	1.1e-02±3.0e-04	1.1e-02±3.0e-04	1.1e-02±3.0e-04	2.9e-02±3.3e-03	1.2e-02±3.0e-04	2.9e-02±3.3e-03
QM8(R1-PBE0.1)	4152.1±159.3	1.8e-02±9.0e-04	1.5e-02±9.0e-04	1.6e-02±2.0e-03	1.4e-02±2.0e-03	1.4e-02±2.0e-03	2.0e-02±1.0e-03	1.7e-02±1.0e-03	1.6e-02±2.3e-03	1.6e-02±2.3e-03	1.6e-02±2.3e-03	1.4e-02±2.0e-03	1.4e-02±2.0e-03	1.4e-02±2.0e-03	4.2e-02±5.9e-03	1.4e-02±2.0e-03	4.2e-02±5.9e-03
QM8(R2-PBE0.1)	4059.8±240.7	3.9e-02±1.0e-03	3.4e-02±1.0e-03	3.4e-02±3.5e-03	1.4e-02±2.9e-03	1.4e-02±2.9e-03	4.1e-02±1.6e-03	3.6e-02±1.7e-03	3.4e-02±3.5e-03	3.4e-02±3.5e-03	3.4e-02±3.5e-03	3.0e-02±2.8e-03	3.0e-02±2.8e-03	3.0e-02±2.8e-03	4.2e-02±5.9e-03	3.0e-02±2.8e-03	4.2e-02±5.9e-03
QM8(E1-PBE0.1)	3932.1±133.8	1.2e-02±2.0e-04	1.1e-02±2.0e-04	1.1e-02±4.0e-04	9.6e-03±3.0e-04	1.3e-02±5.0e-04	1.3e-02±5.0e-04	1.1e-02±4.0e-04	1.1e-02±4.0e-04	1.1e-02±4.0e-04	1.1e-02±4.0e-04	9.6e-03±3.0e-04	1.1e-02±4.0e-04	1.1e-02±4.0e-04	3.1e-02±4.8e-03	1.1e-02±4.0e-04	3.1e-02±4.8e-03
QM8(E2-PBE0.1)	4063.2±133.4	1.3e-02±4.0e-04	1.2e-02±3.0e-04	1.2e-02±6.0e-04	1.1e-02±3.0e-04	1.3e-02±5.0e-04	1.3e-02±5.0e-04	1.2e-02±4.0e-04	1.1e-02±3.0e-04	1.2e-02±4.0e-04	1.1e-02±3.0e-04	1.1e-02±3.0e-04	1.1e-02±3.0e-04	1.1e-02±3.0e-04	2.9e-02±3.3e-03	1.2e-02±3.0e-04	2.9e-02±3.3e-03
QM8(R1-PBE0.1)	4152.1±159.3	1.8e-02±9.0e-04	1.5e-02±9.0e-04	1.6e-02±2.0e-03	1.4e-02±2.0e-03	1.4e-02±2.0e-03	2.0e-02±1.0e-03	1.7e-02±1.0e-03	1.6e-02±2.3e-03	1.6e-02±2.3e-03	1.6e-02±2.3e-03	1.4e-02±2.0e-03	1.4e-02±2.0e-03	1.4e-02±2.0e-03	4.2e-02±5.9e-03	1.4e-02±2.0e-03	4.2e-02±5.9e-03
QM8(R2-PBE0.1)	4059.8±240.7	3.9e-02±1.0e-03	3.4e-02±1.0e-03	3.4e-02±3.5e-03	1.4e-02±2.9e-03	1.4e-02±2.9e-03	4.1e-02±1.6e-03	3.6e-02±1.7e-03	3.4e-02±3.5e-03	3.4e-02±3.5e-03	3.4e-02±3.5e-03	3.0e-02±2.8e-03	3.0e-02±2.8e-03	3.0e-02±2.8e-03	4.2e-02±5.9e-03	3.0e-02±2.8e-03	4.2e-02±5.9e-03
QM8(E1-CAM)	3782.7±252.3	1.1e-02±4.0e-04	1.0e-02±3.0e-04	1.0e-02±3.0e-04	9.1e-03±2.0e-04	1.2e-02±5.0e-04	1.2e-02±5.0e-04	1.1e-02±3.0e-04	1.0e-02±3.0e-04	1.1e-02±3.0e-04	1.0e-02±3.0e-04	9.1e-03±2.0e-04	1.0e-02±3.0e-04	1.0e-02±3.0e-04	2.9e-02±3.3e-03	1.0e-02±3.0e-04	2.9e-02±3.3e-03
QM8(E2-CAM)	4004.4±151.5	1.2e-02±3.0e-04	1.1e-02±3.0e-04	1.1e-02±3.0e-04	1.0e-02±3.0e-04	1.2e-02±5.0e-04	1.2e-02±5.0e-04	1.1e-02±3.0e-04	1.0e-02±3.0e-04	1.1e-02±3.0e-04	1.0e-02±3.0e-04	1.0e-02±3.0e-04	1.0e-02±3.0e-04	1.0e-02±3.0e-04	2.7e-02±3.2e-03	1.1e-02±3.0e-04	2.7e-02±3.2e-03
QM8(R1-CAM)	4125.5±161.7	1.9e-02±1.2e-03	1.6e-02±1.1e-03	1.6e-02±2.0e-03	1.4e-02±1.7e-03	2.2e-02±1.0e-03	2.2e-02±1.0e-03	1.9e-02±1.4e-03	1.8e-02±1.4e-03	1.8e-02±1.4e-03	1.8e-02±1.4e-03	1.6e-02±1.2e-03	1.6e-02±1.2e-03	1.6e-02±1.2e-03	3.1e-02±4.1e-03	1.6e-02±1.2e-03	3.1e-02±4.1e-03
QM8(R2-CAM)	4001.1±224.0	4.1e-02±1.8e-03	3.7e-02±1.3e-03	3.6e-02±3.0e-03	3.2e-02±2.6e-03	4.4e-02±1.2e-03	4.4e-02±1.2e-03	4.0e-02±1.3e-03	3.8e-02±3.0e-03	3.8e-02±3.0e-03	3.8e-02±3.0e-03	3.3e-02±2.8e-03	3.3e-02±2.8e-03	3.3e-02±2.8e-03	5.1e-02±5.8e-03	3.3e-02±2.8e-03	5.1e-02±5.8e-03
QM9(mu)	25845.8±660.3	8.9e-01±5.7e-02	8.1e-01±3.1e-02	8.4e-01±7.7e-02	7.7e-01±2.9e-02	8.7e-01±4.2e-02	8.7e-01±4.2e-02	7.8e-01±2.1e-02	7.9e-01±2.1e-02	7.9e-01±2.1e-02	7.9e-01±2.1e-02	7.8e-01±2.1e-02	7.8e-01±2.1e-02	7.8e-01±2.1e-02	2.1e+00±4.2e-01	7.7e-01±2.0e-02	2.1e+00±4.2e-01
QM9(alpha)	24665.0±1191.1	1.2e+00±3.3e-02	1.1e+00±2.1e-01	1.4e+00±1.3e-01	1.4e+00±1.3e-01	1.2e+00±3.3e-02	1.2e+00±3.3e-02	1.1e+00±2.1e-01	1.1e+00±2.1e-01	1.1e+00±2.1e-01	1.1e+00±2.1e-01	1.1e+00±2.1e-01	1.1e+00±2.1e-01	1.1e+00±2.1e-01	1.4e+01±8.4e-01	1.0e+00±3.3e-02	1.4e+01±8.4e-01
QM9(homo)	26024.3±221.8	7.5e-03±3.0e-04	7.1e-03±3.0e-04	7.4e-03±2.0e-04	7.4e-03±2.0e-04	7.9e-03±2.0e-04	7.9e-03±2.0e-04	6.6e-03±1.0e-04	6.6e-03±1.0e-04	6.6e-03±1.0e-04	6.6e-03±1.0e-04	6.2e-03±1.0e-04	6.2e-03±1.0e-04	6.2e-03±1.0e-04	2.2e+00±1.7e+00	6.6e-03±1.0e-04	2.2e+00±1.7e+00
QM9(lumo)	25608.8±416.6	8.5e-03±2.0e-04	8.1e-03±2.0e-04	8.3e-03±2.0e-04	7.9e-03±3.0e-04	7.9e-03±3.0e-04	7.9e-03±3.0e-04	7.5e-03±2.0e-04	7.5e-03±2.0e-04	7.5e-03±2.0e-04	7.5e-03±2.0e-04	6.2e-03±1.0e-04	6.2e-03±1.0e-04	6.2e-03±1.0e-04	2.1e+00±1.5e+00	7.2e-03±1.0e-04	2.1e+00±1.5e+00
QM9(gap)	25862.9±476.1	1.1e-02±2.0e-04	1.0e-02±2.0e-04	1.1e-02±4.0e-04	9.8e-03±3.0e-04	1.0e-02±5.0e-04	1.0e-02±5.0e-04	9.6e-03±3.0e-04	9.5e-03±3.0e-04	9.5e-03±3.0e-04	9.5e-03±3.0e-04	8.8e-03±3.0e-04	8.8e-03±3.0e-04	8.8e-03±3.0e-04	1.1e+00±5.9e-01	9.4e-03±2.0e-04	1.1e+00±5.9e-01
QM9(r2)	25736.3±537.4	6.3e+01±2.0e+00	5.7e+01±1.6e+00	6.9e+01±2.5e+00	6.2e+01±2.7e+00	5.8e+01±1.9e+00	5.8e+01±1.9e+00	5.2e+01±1.9e+00	5.4e+01±2.7e+00	5.4e+01±2.7e+00	5.4e+01±2.7e+00	4.2e+01±6.1e-01	4.2e+01±6.1e-01	4.2e+01±6.1e-01	2.4e+02±1.1e+01	5.4e+01±9.5e-01	2.4e+02±1.1e+01
QM9(zpve)	24886.6±870.8	1.6e-03±5.0e-04	1.5e-03±1.0e-04	3.8e-03±4.0e-04	3.6e-03±4.0e-04	3.6e-03±4.0e-04	3.6e-03±4.0e-04	2.7e-03±1.0e-04	2.4e-03±1.0e-04	2.4e-03±1.0e-04	2.4e-03±1.0e-04	2.2e-03±1.0e-04	2.2e-03±1.0e-04	2.2e-03±1.0e-04	1.9e+00±1.6e+00	2.4e-03±1.0e-04	1.9e+00±1.6e+00
QM9(u0)	25375.4±499.9	1.9e+00±2.4e-01	1.7e+00±2.1e-01	4.9e+00±6.5e-01	4.2e+00±5.2e-01	3.7e+00±1.4e-01	3.7e+00±1.4e-01	3.2e+00±1.4e-01	3.3e+00±1.3e-01	3.3e+00±1.3e-01	3.3e+00±1.3e-01	2.5e+00±2.8e-02	2.5e+00±2.8e-02	2.5e+00±2.8e-02	4.4e+01±3.7e+00	2.9e+00±1.3e-01	4.4e+01±3.7e+00
QM9(u298)	25204.1±754.3	1.9e+00±2.5e-01	1.7e+00±2.0e-01	4.9e+00±6.9e-01	4.2e+00±5.3e-01	3.7e+00±1.3e-01	3.7e+00±1.3e-01	3.2e+00±1.4e-01	3.3e+00±1.3e-01	3.3e+00±1.3e-01	3.3e+00±1.3e-01	2.5e+00±2.8e-02	2.5e+00±2.8e-02	2.5e+00±2.8e-02	4.4e+01±3.7e+00	2.9e+00±1.3e-01	4.4e+01±3.7e+00
QM9(u298)	25288.9±581.3	1.9e+00±2.4e-01	1.7e+00±2.0e-01	4.9e+00±6.8e-01	4.2e+00±5.3e-01	3.7e+00±1.3e-01	3.7e+00±1.3e-01	3.2e+00±1.4e-01	3.3e+00±1.3e-01	3.3e+00±1.3e-01	3.3e+00±1.3e-01	2.5e+00±2.8e-02	2.5e+00±2.8e-02	2.5e+00±2.8e-02	4.4e+01±3.7e+00	2.9e+00±1.3e-01	4.4e+01±3.7e+00
QM9(g298)	25345.2±543.2	1.9e+00±2.5e-01	1.7e+00±2.0e-01	4.9e+00±6.5e-01	4.2e+00±5.2e-01	3.7e+00±1.3e-01	3.7e+00±1.3e-01	3.2e+00±1.4e-01	3.3e+00±1.3e-01	3.3e+00±1.3e-01	3.3e+00±1.3e-01	2.5e+00±2.8e-02	2.5e+00±2.8e-02	2.5e+00±2.8e-02	4.4e+01±3.7e+00	2.9e+00±1.3e-01	4.4e+01±3.7e+00
QM9(cv)	25051.2±829.4	6.0e+01±2.1e-02	5.5e+01±2.0e-02	6.9e+01±5.5e-02	6.3e+01±4.7e-02	5.7e+01±1.8e-02	5.7e+01±1.8e-02	5.3e+01±2.0e-02	4.9e+01±1.5e-02	4.9e+01±1.5e-02	4.9e+01±1.5e-02	4.4e+01±8.6e-03	4.4e+01±8.6e-03	4.4e+01±8.6e-03	5.2e+00±1.3e+00	4.9e+01±1.5e-02	5.2e+00±1.3e+00
Width @ 90%																	
QM8(EI-CC2)	2373.2±351.0	2.8e-02±2.1e-03	2.7e-02±8.0e-04	2.6e-02±1.4e-03	2.5e-02±9.0e-04	2.9e-02±2.6e-03	2.9e-02±2.6e-03	2.7e-02±8.0e-04	2.5e-02±1.2e-03	2.7e-02±8.0e-04	2.5e-02±1.2e-03	2.4e-02±7.0e-04	2.5e-02±1.2e-03	2.5e-02±1.2e-03	8.4e-02±1.4e-02	2.4e-02±7.0e-04	8.4e-02±1.

Table 14: (On QM9) MCR conditioning on the presence of certain functional groups in the original SMILES representation. The list of groups are taken from the OPENSMILES project, as implemented in [32]. The (pooled) mean coverage rate are computed over 10 random re-splits of the full QM9 dataset like in other parts of this paper. We keep only the functional groups with at least 200 appearances in all ten randomly sampled test set. All numbers not significantly lower than 90% at $p = 0.05$ are in bold.

Conditional Coverage Rate	alpha	cv	g298	gap	h298	homo	lumo	mu	r2	u0	u298	zpve
2-butyne	88.4±0.4	94.6±0.4	93.1±0.4	94.9±0.4	92.8±0.4	95.6±0.4	94.4±0.4	94.3±0.4	93.2±0.4	92.8±0.4	93.0±0.4	92.2±0.4
aldehyde	93.3±0.4	94.4±0.4	94.8±0.4	92.6±0.4	94.4±0.4	94.7±0.4	91.1±0.4	90.7±0.4	90.4±0.4	94.4±0.4	94.6±0.4	93.6±0.4
amide	89.7±0.3	89.7±0.3	90.0±0.3	91.1±0.3	90.6±0.3	92.2±0.3	89.9±0.3	88.0±0.3	91.4±0.3	90.3±0.3	90.2±0.3	90.3±0.3
carboxylic acid	91.9±0.4	93.2±0.4	90.0±0.4	91.4±0.4	89.7±0.4	92.3±0.4	92.4±0.4	92.7±0.4	91.8±0.4	90.0±0.4	90.0±0.4	91.1±0.4
cyclopropane	89.9±0.3	90.5±0.3	93.5±0.3	90.9±0.3	93.7±0.3	89.8±0.3	91.8±0.3	93.1±0.3	88.7±0.3	93.6±0.3	93.8±0.3	91.2±0.3
dimethyl ether	90.4±0.1	91.9±0.1	89.4±0.1	91.6±0.1	89.3±0.1	91.9±0.1	91.5±0.1	92.2±0.1	88.7±0.1	89.3±0.1	89.4±0.1	90.6±0.1
ester	92.5±0.6	94.0±0.6	90.8±0.6	90.2±0.6	90.2±0.6	91.5±0.6	91.4±0.6	91.9±0.6	92.3±0.6	90.3±0.6	90.6±0.6	92.3±0.6
ethanol	90.0±0.2	92.0±0.2	90.0±0.2	93.1±0.2	90.1±0.2	92.9±0.2	92.5±0.2	91.8±0.2	88.1±0.2	90.0±0.2	90.1±0.2	90.8±0.2
ethene	84.1±0.2	89.5±0.2	86.7±0.2	90.3±0.2	86.9±0.2	91.4±0.2	89.3±0.2	92.8±0.2	90.0±0.2	86.7±0.2	86.8±0.2	87.0±0.2
ether	90.4±0.1	91.9±0.1	89.4±0.1	91.6±0.1	89.3±0.1	91.9±0.1	91.5±0.1	92.2±0.1	88.7±0.1	89.3±0.1	89.4±0.1	90.6±0.1
formaldehyde	90.3±0.2	91.5±0.2	91.9±0.2	90.9±0.2	92.0±0.2	91.7±0.2	89.7±0.2	86.7±0.2	88.3±0.2	91.9±0.2	91.9±0.2	91.5±0.2
hydrogen cyanide	93.8±0.2	93.7±0.2	93.4±0.2	89.9±0.2	93.4±0.2	89.6±0.2	92.1±0.2	88.3±0.2	92.2±0.2	93.3±0.2	93.1±0.2	91.6±0.2
ketone	88.7±0.3	90.9±0.3	89.4±0.3	92.2±0.3	89.5±0.3	91.5±0.3	90.7±0.3	90.6±0.3	90.7±0.3	89.7±0.3	89.8±0.3	89.8±0.3
prop-1-ene	84.5±0.3	89.6±0.3	85.2±0.3	90.4±0.3	85.6±0.3	92.5±0.3	89.3±0.3	94.1±0.3	89.3±0.3	85.3±0.3	85.5±0.3	86.1±0.3
prop-1-yne	89.8±0.3	94.8±0.3	94.0±0.3	94.6±0.3	93.6±0.3	95.4±0.3	94.0±0.3	94.4±0.3	92.2±0.3	93.8±0.3	93.8±0.3	92.8±0.3

C Discussion on Discriminative Jackknife

Discriminative Jackknife (DJ) was recently proposed as a post-hoc method to construct prediction intervals for regression deep learning models [1]. [1] claims that DJ is simultaneously marginally valid and discriminative. Unfortunately, *neither claim is true*, and it has other practical issues, as we will discuss in detail in this section.

C.1 Jackknife+ vs. DJ

Although it is out-of-scope for this paper, we would like to briefly explain where the finite-sample coverage guarantee comes from, or rather *should have* come from. It is highly recommended that the readers read the original work of Jackknife+, [4] which lays the theoretical foundation for [1] more details.

Suppose we have training data $\{Z_i\}_{i=1}^n$ where $Z_i = (X_i, Y_i)$, and $(X, Y) \sim \mathcal{P}$ for some unknown distribution \mathcal{P} . Suppose we have an *order-invariant* algorithm \mathcal{A} that trains a mean-estimator given some data. We will denote the full estimator as $\hat{\mu}$, the leave-one-out (LOO) estimator as $\hat{\mu}_{-i}$, and the LOO residual as R_i^{LOO} , defined as:

$$\hat{\mu} := \mathcal{A}(\{(X_j, Y_j)\}_{j \in [n]}) \quad (24)$$

$$\hat{\mu}_{-i} := \mathcal{A}(\{(X_j, Y_j)\}_{j \in [n] \setminus \{i\}}) \quad (25)$$

$$R_i^{LOO} := |Y_i - \hat{\mu}_{-i}(X_i)| \quad (26)$$

We will also define $\hat{q}_{n,\beta}^+\{v_i\}$ as the $\lceil (n+1)\beta \rceil$ -th smallest (close to the β -th quantile) of v_1, \dots, v_n , and $\hat{q}_{n,\beta}^-\{v_i\}$ as the $\lfloor (n+1)\beta \rfloor$ smallest value¹⁰.

The original Jackknife+ [4] does the following to construct a PI with finite-sample coverage guarantee (at level $1 - 2\alpha$, but empirically usually covers $1 - \alpha$ of the time):

- Step 1: Train the LOO estimator $\hat{\mu}_{-i}$ for $i \in [n]$.
- Step 2: Collect the LOO residuals R_i^{LOO} for $i \in [n]$.
- Step 3 (inference): For a new data point (X_{n+1}, Y_{n+1}) , the Jackknife+ PI would be

$$\hat{C}_\alpha^{Jackknife+}(X_{n+1}) := [\hat{q}_{n,\alpha}^-\{\hat{\mu}_{-i}(X_{n+1}) - R_i^{LOO}\}, \hat{q}_{n,1-\alpha}^+\{\hat{\mu}_{-i}(X_{n+1}) + R_i^{LOO}\}] \quad (27)$$

Assuming exchangeability of $\{Z_i\}_{i=1}^{n+1}$, [4] proves that

$$\mathbb{P}\{Y_{n+1} \in \hat{C}_\alpha^{Jackknife+}(X_{n+1})\} \geq 1 - 2\alpha \quad (28)$$

Here the probability is taken over all training samples and the test data.

DJ aims to apply the above for deep learning algorithm \mathcal{A} . The only difference between DJ and Jackknife+ is that replaces step 1 with step 1b below:

- Step 1b: replace $\hat{\mu}_{-i}$ with $\hat{\mu}_{-i}^{HOIF}$, which is estimated using $\hat{\mu}$ and higher-order influence function (HOIF) without actually retraining the deep learning algorithm \mathcal{A} .

C.2 Validity

Although using influence function (IF) to estimate $\hat{\mu}_{-i}$ is possible, in practice, there is almost no way to do this. For the coverage guarantee (Theorem 1 in [4]) to hold, it is important that for $\hat{\mu}_{-i}$, Z_i and Z_{n+1} are also “exchangeable”. In other words, $\hat{\mu}_{-i}$ cannot see Z_i at all, which is crucial in Step 2 of the proof of Theorem 1 (Section 6 in [4]). If $\hat{\mu}_{-i}$ actually “remember” Z_i somehow, then the last step of Step 2 in the proof breaks.

Unfortunately, $\hat{\mu}_{-i}^{HOIF}$ does “remember” the Z_i it saw. The original paper [18] also uses IF to estimate the LOO models, but it only applies this to understand which training sample has more influence on the model, or in some qualitative assessment settings (as the name of the paper suggests). Even for such use case, [6] summarizes several issues with using IF in deep learning, one of which

¹⁰Note the $+$ and $-$ signs are used to distinguish the $\lceil \cdot \rceil$ and $\lfloor \cdot \rfloor$ operations.

is the error in estimating just the ranking of the influences even with first order IF estimated with *exact* inverse-Hessian vector product (HVP). In [1], the HOIFs are computed recursively, and every IF is computed with *approximate* HVP, which means there is little understanding in the quality of such estimates¹¹. To actually achieve the theoretical guarantee in this setting, we need to eliminate completely the influence of Z_i on the model parameters of $\hat{\mu}$, which requires infinite-order exact IF and is clearly unrealistic.

C.3 Discrimination

The short answer to this is DJ is actually not discriminative, or at least not in practice. This can be found in our experiments in Section 4.2. [1] reports high AUPRC due to a code error¹². It is worth noting that the exact version of Jackknife+ does not show discrimination in the way claimed in [1] either (See the comparison in Figure 3). The varying width of the PI is a by-product of the

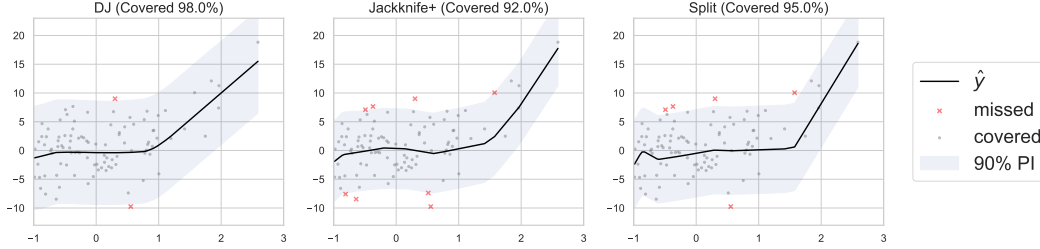


Figure 3: DJ, Jackknife+ and Split conformal on the synthetic dataset.

construction and proof, and is usually close to constant in practice. Intuitively, as $n \rightarrow \infty$, $\hat{\mu}_{-i} \rightarrow \hat{\mu}$, and the variance of the PI width would $\rightarrow 0$. Here are two simple thought experiments:

1. As $n \rightarrow \infty$, $\hat{\mu}_{-i} \rightarrow \hat{\mu}$, and the variance of the PI width would $\rightarrow 0$.
2. Suppose X follows a uniform distribution from $\{-10, -9, \dots, 0, \dots, 9, 10\}$, and $Y = |X|$. Suppose \mathcal{A} is a linear regression algorithm without intercept. As long as n is big enough, the PI for any input X_{n+1} would be $[-9, 9]$. The error would however $\rightarrow |X_{n+1}|$ (because $\hat{\mu}(x) \rightarrow 0$), so there is not discrimination at all.

As a result, DJ, the approximated version, could only potentially be discriminative due to some numerical instability and/or some effect that is orthogonal to the LOO procedure and the construction of the PI, which requires more exploration and detailed explanation.

C.4 Other Considerations

Order-invariance for \mathcal{A} is rarely satisfied for the deep learning model. This is because a deep learning model usually uses some variants of stochastic gradient descent (SGD) instead of gradient descent, which means permuting the input data would result in different $\hat{\mu}$. However, it is also required for the proof in [4]. [1] did not mention this at all, which results in an incomplete proof even if every stated above is fixed. That said, the proof [4] could easily be extended to training DNN with SGD as well; however it is out of the scope of this discussion.

Scalability of the proposed method in DJ is not practical, even the employed approximations. At training time, at least for the experiments in [1], directly performing the LOO procedure is faster than actually computing influence functions and estimating $\hat{\mu}_{-i}$. This of course depends on the number of training data points vs. the number of parameters of the DNN. However, as we will discuss in Section C.5, there is no strong argument for using DJ in any scenario. Moreover, if we do not store all the LOO model weights (which has a large space requirement), we would need to compute the IFs on the fly for each test data, which is prohibitively expensive.

Stability is another concern. In using the influence function, inverting Hessian is very expensive, so DJ follows [18] in using a stochastic Hessian Vector Product (HVP) method. However, one would

¹¹In fact, based on the experiment, the errors seem to build up, as we will discuss in Section C.3.

¹²https://github.com/ahmedmalaa/discriminative-jackknife/blob/e012d0a359aa8dac16fe03a99fa586966cf86ffe/UCI_experiments.py#L82

also need to get a good estimate of the eigenvalue of the Hessian¹³ for the HVP estimation process to converge meaningfully. In our experiment (and in the code published by the authors of [1]), exact Hessian with small NNs have to be used, instead of HVP, due to stability issues.

C.5 Conclusion

If we take a step back, Jackknife+ was proposed as an improved version of the classical Jackknife with a finite-sample marginal coverage guarantee. The question it tries to address however is not just concerning finite-sample marginal coverage, but also about data scarcity: As noted in the original Jackknife+ paper [4], split conformal already has a finite-sample guarantee (at $1 - \alpha$ level as opposed to $1 - 2\alpha$ of Jackknife+), but the limitation is that it requires reserving a hold-out set. When the model requires more data to train, this might result in a poor fit. Of course, it is desirable to use all the data we have to train the base model. However, in many cases we only need a small portion of the data as the validation/calibration set. If data is abundant, this is not a concern, so one could use split conformal (or CQR, MADSplit, LVD, etc.). If the data is actually very scarce, then usually the model cannot be too complicated, so directly performing the LOO cross-validation with Jackknife+ would not be too expensive and will keep the theoretical guarantee. If we use DJ, we might spend more time while breaking the theoretical guarantee.

¹³which can be very large and thus unstable to estimate according to [6]

D Data

In this section, we will try our best to list the licenses of the public datasets we use and details about how the consent was obtained.

- UCI Yacht Hydrodynamics (Yacht)[38]: We could not find the license for this dataset. The dataset was created by “Ship Hydromechanics Laboratory, Maritime and Transport Technology Department, Technical University of Delft”, and donated by “Dr Roberto Lopez” per [38].
- UCI Bikesharing (Bike) [35, 10]: The original data was provided according to the Capital Bikeshare Data License Agreement <https://www.capitalbikeshare.com/data-license-agreement>. We could not find details on how the data was obtained.
- UCI Energy Efficiency (Energy)[37, 34]: We could not find the license for this dataset. The dataset was created by Angeliki Xifara (angxifara '@' gmail.com, Civil/Structural Engineer) and was processed by Athanasios Tsanas (tsanasthanasis '@' gmail.com, Oxford Centre for Industrial and Applied Mathematics, University of Oxford, UK).
- UCI Concrete Compressive Strength (Concrete)[36, 46]: We could not find the license for this dataset. The dataset was original owned and donated by Prof. I-Cheng Yeh at Department of Information Management at Chung-Hua University, Taiwan, R.O.C.
- Boston Housing (Housing)[9]: We could not find the license for this dataset. This dataset contains information collected by the U.S Census Service concerning housing in the area of Boston Mass¹⁴.
- Kin8nm[16]: We could not find the license for this dataset. The original parent dataset (the “kin” dataset) was contributed by Zoubin Ghahramani¹⁵.
- QM8 [28, 30] and QM9 [30, 27]: We could not find the original license for these datasets, but they are discribed under CC By 4.0¹⁶. They are obtained in [28] and [27].

¹⁴<https://www.cs.toronto.edu/delve/data/boston/bostonDetail.html>

¹⁵<https://www.cs.toronto.edu/delve/data/kin/desc.html>

¹⁶https://tdcommons.ai/single_pred_tasks/qm/